Biomedicine & Pharmacotherapy 177 (2024) 116867

Contents lists available at ScienceDirect

Biomedicine & Pharmacotherapy

journal homepage: www.elsevier.com/locate/biopha

Non-hallucinogenic compounds derived from iboga alkaloids alleviate neuropathic and visceral pain in mice through a mechanism involving 5-HT_{2A} receptor activation

Hugo R. Arias [a,1], Laura Micheli [b,*,1], Deborah Rudin [c,d], Ophelie Bento [e], Saskia Borsdorf [f], Clara Ciampi [b], Philippe Marin [e], Evgeni Ponimaskin [f], Dina Manetti [g], Maria Novella Romanelli [g], Carla Ghelardini [b], Matthias E. Liechti [c,d], Lorenzo Di Cesare Mannelli [b]

[a] Department of Pharmacology and Physiology, College of Osteopathic Medicine, Oklahoma State University Center for Health Sciences, Tahlequah, OK, USA
[b] Department of Neurosciences, Psychology, Drug Research and Child Health (NEUROFARBA), Section of Pharmacology and Toxicology, University of Florence, Florence, Italy
[c] Division of Clinical Pharmacology and Toxicology, Department of Biomedicine, University Hospital Basel, Basel, Switzerland
[d] Division of Clinical Pharmacology and Toxicology, Department of Pharmaceutical Sciences, University of Basel, Basel, Switzerland
[e] Institut de Génomique Fonctionnelle, Université de Montpellier, CNRS, INSERM, Montpellier, France
[f] Cellular Neurophysiology, Hannover Medical School, Hannover, Germany
[g] Section of Pharmaceutical and Nutraceutical Sciences, University of Florence, Florence, Italy

ARTICLE INFO

Key words:
Visceral pain
neuropathic pain
ibogalogs
agonist and reverse agonist
5-HT_{2A}
5-HT_6
and 5-HT_7 receptors

ABSTRACT

The aim of this study was to determine the anti-hypersensitivity activity of novel non-hallucinogenic compounds derived from iboga alkaloids (i.e., ibogalogs), including tabernanthalog (TBG), ibogainalog (IBG), and ibogaminalog (DM506), using mouse models of neuropathic (Chronic Constriction Injury; CCI) and visceral pain (dextrane sulfate sodium; DSS). Ibogalogs decreased mechanical hyperalgesia and allodynia induced by CCI in a dose- and timeframe-dependent manner, where IBG showed the longest anti-hyperalgesic activity at a comparatively lower dose, whereas DM506 displayed the quickest response. These compounds also decreased hypersensitivity induced by colitis, where DM506 showed the longest activity. To understand the mechanisms involved in these effects, two approaches were utilized: ibogalogs were challenged with the 5-HT_{2A} receptor antagonist ketanserin and the pharmacological activity of these compounds was assessed at the respective 5-HT_{2A}, 5-HT_6, and 5-HT_7 receptor subtypes. The behavioral results clearly demonstrated that ketanserin abolishes the pain-relieving activity of ibogalogs without inducing any effect *per se*, supporting the concept that 5-HT_{2A} receptor activation, but not inhibition, is involved in this process. The functional results showed that ibogalogs potently activate the 5-HT_{2A} and 5-HT_6 receptor subtypes, whereas they behave as inverse agonists (except TBG) at the 5-HT_7 receptor. Considering previous studies showing that 5-HT_6 receptor inhibition, but not activation, and 5-HT_7 receptor activation, but not inhibition, relieved chronic pain, we can discard these two receptor subtypes as participating in the pain-relieving activity of ibogalogs. The potential involvement of 5-$HT_{2B/2C}$ receptor subtypes was also ruled out. In conclusion, the anti-hypersensitivity activity of ibogalogs in mice is mediated by a mechanism involving 5-HT_{2A} receptor activation.

Abbreviations: CCI, chronic constriction injury; CRD, colorectal distension; AWR, abdominal withdrawal reflex; DSS, dextran sodium sulphate; TBG tabernanthalog, 8-methoxy-3-methyl-1,2,3,4,5,6-hexahydroazepino[4,5-*b*]indole fumarate; IBG ibogainalog, 9-methoxy-3-methyl-1,2,3,4,5,6-hexahydroazepino[4,5-*b*] indole hydrochloride; DM506 ibogaminalog, 3-methyl-1,2,3,4,5,6-hexahydroazepino[4,5-*b*]indole fumarate; NAChR, nicotinic acetylcholine receptor; 5-HT_{2A}, serotonin 2 A receptor subtype; 5-HT_{2B}, serotonin 2B receptor subtype; 5-HT_{2C}, serotonin 2 C receptor subtype; 5-HT_6, serotonin 6 receptor subtype; 5-HT_7, serotonin 7 receptor subtype; $Ca_V2.2$, voltage-gated N-type calcium channel; CNS, central nervous system; RT, room temperature; HTRF, Homogeneous Time-Resolved Fluorescence; IP1, inositol monophosphate 1; BRET, bioluminescence resonance energy transfer; FRET, fluorescence resonance energy transfer; EC_{50}, ligand concentration that produces 50 % activation; IC_{50}, ligand concentration that produces 50 % inhibition; E_{max} efficacy, maximal agonistic activity.

* Corresponding author.
E-mail address: laura.micheli@unifi.it (L. Micheli).
[1] Hugo R. Arias and Laura Micheli contributed equally to this work.

https://doi.org/10.1016/j.biopha.2024.116867
Received 29 March 2024; Received in revised form 28 May 2024; Accepted 3 June 2024

1. Introduction

Chronic pain conditions refer to a range of multifaceted and complex disorders that involve millions of people worldwide determining significant burden on society, health care system and personal well-being [1]. Chronic pain management represents a hard challenge for researchers and clinicians since there is no universally effective treatment and often the therapies must be continued for a long period [2]. The WHO indicated that therapies for the management of mild-to-severe chronic pain such as nonsteroidal anti-inflammatory drugs or opioids are not free from several side effects [3]. Thus, new therapeutic approaches are needed for a more effective and safe approach to pain management.

Mounting evidence indicates that several metabotropic serotonin (5-HT) receptor subtypes are involved in pain processing in physiological and pathological conditions (reviewed in [4–6]). However, there is still controversy whether activation or inhibition of the 5-HT_{2A} receptor reduces pain using a variety of animal models. It has been suggested that activation of either the 5-HT_{2A} or 5-HT_{2C} receptor produces anti-allodynic effects *via* different spinal mechanisms [7]. On the other hand, the activation of the 5-HT_7 receptor induces antinociceptive and anti-inflammatory effects using a variety of pain models [8–10]. In addition, inverse agonist-induced 5-HT_6 receptor inhibition showed anti-neuropathic activity in different pain models [11–13].

Novel non-hallucinogenic derivatives of iboga alkaloids (so called "ibogalogs"), including ibogainalog (IBG), tabernanthalog (TBG), and ibogaminalog (DM506) (see molecular structures in Fig. 1) induced antiaddictive, antidepressant- and anxiolytic-like activity in rodents, and the main mechanism has been attributed to 5-HT_{2A} receptor activation [14–16]. Nevertheless, there is no study showing that ibogalogs may decrease neuropathic pain and/or allodynia in rodents, and the potential targets and mechanisms involved.

We determined, in this work, the effect of TBG, IBG, and DM506 using both visceral [17] and chronic constriction injury (CCI) [18] mouse models of persistent pain. Neuropathic pain, a type of chronic pain, arises as result of an injury to the peripheral and/or central nervous system (CNS) involved in the propagation of pain-related signals from nociceptors to the brain [19]. Visceral pain is a nociceptive phenomenon characterized by non-localized pain of unclear etiology originated in thoracic or abdominal visceral organs [20,21]. Both types of pain are marked by central sensitization, related in general to a maladaptive plasticity of the CNS induced by persistent pathological pain. Since ibogalogs modulate a variety of 5-HT receptors [14,16], different receptor subtypes might be involved in the studied pain-relieving activity. To begin evaluating potential molecular mechanisms, two approaches were utilized: the pain-relieving activity of TBG, IBG, and DM506 was challenged with ketanserin, a potent antagonist of the 5-HT_{2A} receptor [14,22–24], and the pharmacological profile of these compounds was compared among 5-HT_{2A}, 5-HT_6, and 5-HT_7 receptor subtypes using functional assays.

2. Material and methods

2.1. Material

Neuroblastoma x glioma hybrid NG108–15 cells and murine neuroblastoma N1E-115 cells were obtained from American Type Culture Collection (ATCC®) (Virginia, USA). NIH/3T3 cells and serotonin hydrochloride (5-HT) were obtained from Merck (Buchs, Switzerland). WAY181,187 oxalate, SB-269970 hydrochloride, and 5-carboxamidotryptamine maleate (5-CT) were obtained from Tocris (Noyal Châtillon sur Seiche, France; Wiesbaden-Nordenstadt, Germany). Ketanserin tartrate and penicillin/streptomycin were purchased from Merck (Milan, Italy; Darmstadt, Germany). Intepirdine, 3-isobutyl-1-methylxanthine (IBMX), and Tween 20 were purchased from Sigma (Saint Quentin Fallavier, France; Munich, Germany). Coelanterazine H and Lipofectamine 2000 were purchased from ThermoFisher Scientific (Courtaboeuf, France; Zug, Switzerland). Dextran sodium sulphate (MW 36000–50000 Da) was purchased from AbMole Bioscience (Brussels, Belgium). The HTRF IP-One G_q Detection kit was obtained from Revvity (Schweiz) AG (Zurich, Switzerland). White 96-well plates were purchased from Greiner Bio-One (Les Ulis, France). Dulbecco's Modified Eagle Medium (DMEM) and Opti-MEM medium were obtained from Gibco Life Technologies (CA, USA). Fetal bovine serum (FBS) was purchased from Biochrom Ltd. (Cambridge, UK). TBG fumarate and IBG hydrochloride were synthesized by AmBeed (Arlington Heights, IL,

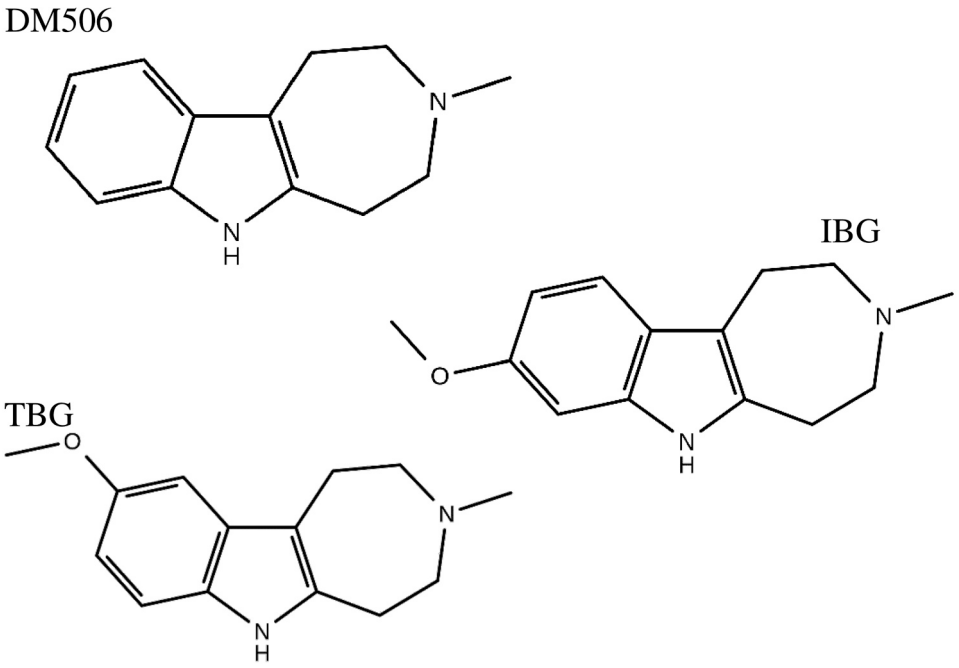

Fig. 1. Molecular structure of DM506 (3-methyl-1,2,3,4,5,6-hexahydroazepino[4,5-*b*]indole), IBG (9-methoxy-3-methyl-1,2,3,4,5,6-hexahydroazepino[4,5-*b*]indole), and TBG (8-methoxy-3-methyl-1,2,3,4,5,6-hexahydroazepino[4,5-*b*]indole).

USA), based on the procedure described previously [14]. DM506 (base) was synthesized as described elsewhere [16]. Salts and solvents were of analytical grade.

2.2. Animals

Male CD-1 albino mice (used in the CCI mouse model) and male C57BL/6 N mice (used in the DSS mouse model) (2–3 months old; 22–25 g) (Envigo, Varese, Italy) were housed in CeSAL (Centro Stabulazione Animali da Laboratorio, University of Florence) and used at least 1 week after their arrival. Mice (ten/cage; size 26 × 41 cm) were fed a standard laboratory diet and tap water *ad libitum* and kept at 23 ± 1 °C with a 12 h light/dark cycle, light at 7 am. All animal manipulations were carried out according to the Directive 2010/63/EU of the European parliament and of the European Union council (September 22, 2010) on the protection of animals used for scientific purposes. Formal approval to conduct animal experiments was obtained from the Animal Subjects Review Board of the University of Florence, in compliance with the Guide for the Care and Use of Laboratory Animals of the NIH (USA). All efforts were made to minimize animal suffering and to reduce the number of animals used. A randomization of animals between groups and treatments was carried out. The investigators responsible for data analysis were blind to which animals represent treatments and controls.

2.3. Behavioral study

2.3.1. Toxicological test

Toxicity was evaluated in mice according to Irwin [27] after a single administration of TBG fumarate (40 and 80 mg/kg), IBG hydrochloride (3 and 15 mg/kg), or DM506 (base) (15 and 40 mg/kg) (solubilized with 5 % DMSO and 5 % Tween 20 in saline solution). Following drug administration, animals (n = 4) were observed during 24 h for signs of behavioral, autonomic, and neurological manifestations, including motor displacement, motor reflexes, stereotypes, grooming, reaction to painful or environmental stimuli (analgesia, irritability), startle response, secretions, excretions, respiratory movements, skin color and temperature, piloerection, exophthalmia (exaggerated protrusion of the eyeball), eyelid and corneal reflexes, ataxia, tremors, head twitches, jumps, convulsions, and Straub tail. For postural reflexes (righting reflex) and other signs such as piloerection, exophthalmia, ataxia, tremors, and Straub tail, only the presence or absence was recorded. All signs were evaluated semi-quantitatively, according to the Irwin's scale, with few modifications: spontaneous activity, curiosity, reactivity, straightening reflex and palpebral opening were scored from 4 (normal) to 0 (absent), passivity, vocalization, Straub tail, tremors, convulsions, piloerection, cyanosis, flushing, pallor and writhing were scored from 0 (normal) to 4 (maximum), hypo/hyperthermia were scored from −4 (severe hypothermia) to +4 (severe hyperthermia), and exophthalmos, salivation, lacrimation, immediate death and delayed death were scored as 0 (absent) or + (present). Sedation expresses the final interpretation of a group of signs, including reduced motor activity, reduced startle response, eyelid ptosis, and reduced response to manual manipulation, whereas CNS excitability is considered when increased motor activity, increased startle response, increased response to manual manipulation, and exophthalmia is observed. Hyperactivity includes running, jumps, and attempts to escape from the container. Trained observers not informed about the specific treatment of each animal group carried out this test.

2.3.2. Chronic constriction Injury (CCI)-induced neuropathic pain

CCI to the sciatic nerve of the mouse right hind leg was performed under general anesthesia using the well-characterized Bennett and Xie model [18], with minor modifications. Briefly, animals (weighing 25–30 g at the time of surgery) were anesthetized with 2 % isoflurane/O_2 inhalation and maintained under anesthesia for the duration of surgery. The left thigh was shaved and a small incision (1–1.5 cm in length) was made in the middle of the lateral aspect of the left thigh to expose the sciatic nerve. The nerve was loosely ligated around the entire diameter of the nerve at 3 distinct sites (spaced 1 mm apart) using silk sutures (6.0). The surgical site was closed with a single muscle suture and a skin clip. Pilot studies established that under our experimental conditions, the peak of mechano-allodynia develops by day 5–7 following CCI. Test compounds or used vehicles were administered at the peak of mechanical allodynia (day 8–9) [28]. Sham (control) animals were subjected to surgery in which sciatic nerve was only exposed but not ligated.

2.3.3. Dextran Sodium Sulphate (DSS)-induced visceral pain model

Experimental colitis was induced in mice by giving them 2.5 % dextran sodium sulphate (DSS) (w:v) in tap water *ad libitum* from day 0 until day 5, followed by DSS-free water in the next three days. Treatment with each compound was performed on day 8, after three days of washout from DSS assumption, as described previously [17], with minor modification.

2.3.4. Drug treatments

TBG fumarate (15 and 40 mg/kg) and IBG hydrochloride (3 mg/kg) were dissolved in 0.9 % NaCl (saline) solution, whereas DM506 (base) (5 and 15 mg/kg) was solubilized with 5 % DMSO and 5 % Tween 20 in saline solution. The used doses were chosen based on the toxicological activity of each compound (Table 1) as well as on previous behavioral results [14–16,25]. Each compound or vehicle was intraperitoneally (i.p.) administered using equal volume (10 mL/kg). In the CCI pain model, the Paw pressure and von Frey tests were respectively assessed before (0 min) and after treatment (at 15, 30, 60, 90 min, and 24 h, respectively). In the visceral pain model, abdominal withdrawal reflex measurements were assessed before (0 min) and after treatment (at 30, 60, 90, and 240 min, respectively). To determine whether the 5-HT_{2A} receptor is involved in the behavioral effects of ibogalogs, the potent antagonist ketanserin (1 mg/kg; dissolved in saline solution) [16,22] was administered (i.p.) 30 min before each ibogalog, or vehicle.

2.3.5. Paw pressure test

Mechanical hyperalgesia was determined by measuring the latency to withdraw (in sec) the paw away from a constant mechanical pressure (i.e., noxious stimulus) exerted onto the dorsal surface of the paw [29]. A 15-g calibrated glass cylindrical rod (diameter = 10 mm) chamfered to a conical point (diameter = 3 mm) was used to exert the mechanical force. The weight of the instrument used to apply the force on the paw's animal was suspended vertically between two rings attached to a stand and the mouse was free to move vertically. A single measure was made per animal. A cut-off time of 40 s was used [30,31].

2.3.6. von Frey test

Mechanical allodynia was determined by measuring the withdrawal threshold after a non-noxious stimulus. Animals were placed in plexiglass boxes (20 cm × 20 cm) equipped with a metallic mesh floor, 20 cm above the bench. Habituation of 15 min was allowed before the test. The pain sensitivity threshold was evaluated by applying force ranging from 0 to 5 g with 0.2 g accuracy using an electronic von Frey hair unit (Ugo Basile, Varese, Italy). Punctate stimulus was delivered to the mid-plantar area of each ipsilateral (injured) hindpaw from below the mesh floor through a plastic tip and the withdrawal threshold was automatically displayed on the screen. Paw sensitivity threshold was defined as the minimum pressure required to elicit a robust and immediate withdrawal reflex of the ipsilateral hindpaw. The obtained values were compared to that in the contralateral (uninjured) hindpaw. Voluntary movements associated with locomotion were not taken as a withdrawal response. Stimuli were applied on each anterior paw with an interval of 5 s. The measure was repeated five times, and the final value was obtained by averaging the 5 measures [32].

Table 1
Toxicological profile of TBG, IBG, and DM506 at different doses based on the Irwin test.

Test	TBG		IBG		DM506		Score
	40 mg/kg	80 mg/kg	3 mg/kg	15 mg/kg	15 mg/kg	40 mg/kg	
Behavior							
Spontaneous activity	4 ± 0	1 ± 0	4 ± 0	2 ± 0	4 ± 0	2 ± 0	4 / 0
Passivity	0 ± 0	3 ± 0	0 ± 0	3 ± 0	0 ± 0	2 ± 0	0 / 4
Curiosity	4 ± 0	1 ± 0	4 ± 0	1 ± 0	4 ± 0	2 ± 0	4 / 0
Reactivity	4 ± 0	1 ± 0	4 ± 0	2 ± 0	4 ± 0	2 ± 0	4 / 0
Vocalization	0 ± 0	0 ± 0	0 ± 0	0 ± 0	0 ± 0	0 ± 0	0 / 4
Central Nervous System excitability							
Straub tail	0 ± 0	0 ± 0	0 ± 0	0 ± 0	0 ± 0	0 ± 0	0 / 4
Tremors	0 ± 0	3 ± 0	0 ± 0	3 ± 0	0 ± 0	0 ± 0	0 / 4
Convulsions	0 ± 0	1 ± 0	0 ± 0	0 ± 0	0 ± 0	0 ± 0	0 / 4
Movement							
Ataxia	0 ± 0	0 ± 0	0 ± 0	0 ± 0	0 ± 0	0 ± 0	0 / 4
Stereotypes	0 ± 0	0 ± 0	0 ± 0	0 ± 0	0 ± 0	0 ± 0	0 / 4
Straightening reflex	4 ± 0	3 ± 0	4 ± 0	4 ± 0	4 ± 0	4 ± 0	4 / 0
Autonomic signs							
Piloerection	0 ± 0	0 ± 0	0 ± 0	0 ± 0	0 ± 0	0 ± 0	0 / 4
Exophthalmos	0 ± 0	0 ± 0	0 ± 0	0 ± 0	0 ± 0	0 ± 0	0 / +
Cyanosis	0 ± 0	0 ± 0	0 ± 0	0 ± 0	0 ± 0	0 ± 0	0 / 4
Flushing	0 ± 0	0 ± 0	0 ± 0	0 ± 0	0 ± 0	0 ± 0	0 / 4
Pallor	0 ± 0	0 ± 0	0 ± 0	0 ± 0	0 ± 0	0 ± 0	0 / 4
Palpebral opening	4 ± 0	3 ± 0	4 ± 0	2 ± 0	4 ± 0	4 ± 0	4 / 0
Salivation	0 ± 0	0 ± 0	0 ± 0	0 ± 0	0 ± 0	0 ± 0	0 / +
Lacrimation	0 ± 0	0 ± 0	0 ± 0	0 ± 0	0 ± 0	0 ± 0	0 / +
Hypo/hyperthermia	0 ± 0	2 ± 0	0 ± 0	2 ± 0	0 ± 0	0 ± 0	-4/+4
Writhing	0 ± 0	0 ± 0	0 ± 0	0 ± 0	0 ± 0	0 ± 0	0 / 4
Lethality							
Immediate death	0 ± 0	0 ± 0	0 ± 0	0 ± 0	0 ± 0	0 ± 0	0 / +
Delayed death (48 h)	0 ± 0	0 ± 0	0 ± 0	0 ± 0	0 ± 0	0 ± 0	0 / +

Score: spontaneous activity, curiosity, reactivity, straightening reflex and palpebral opening (normal = 4, absent = 0); passivity, vocalization, straub tail, tremors, convulsions, piloerection, cyanosis, flushing, pallor and writhing (normal = 0, maximum = 4); hypo/hyperthermia (severe hypothermia = −4, severe hyperthermia = +4), and exophthalmos, salivation, lacrimation, immediate death and delayed death (absent = 0 or present = +). Data are expressed as mean ± SEM.

2.3.7. Assessment of visceral sensitivity by Abdominal Withdrawal Reflex (AWR)

Visceral sensitivity to colorectal distension (CRD) was assessed *via* Abdominal Withdrawal Reflex (AWR) measurement using a semi-quantitative score as described previously in conscious animals [33]. Briefly, mice were anaesthetized with isoflurane (2 %) as previously described, and a lubricated latex balloon (length: 4.5 cm), attached to polyethylene tubing, assembled to an embolectomy catheter, and connected to a syringe filled with water, was inserted through the anus into the rectum and descending colon of adult mice. The tubing was taped to the tail to hold the balloon in place. Then, mice were allowed to recover from anesthesia for 15 min. The AWR measurement consisted of visual observation of animal responses to increased volumes (i.e., 50, 100, 150, 200 μL) which produce colorectal distention, and consequently pain. Measurements were performed every 30 min in which the response to graded CRD from 50 μL to 200 μL was evaluated. A blinded observer assigned a score depending on these specific behaviors: score 0: no behavioral response to colorectal distention; score 1: immobile during colorectal distention and occasional head clinching at stimulus onset; score 2: mild contraction of the abdominal muscles but absence of abdomen lifting from the platform; score 3: strong contraction of the abdominal muscles and lifting of the abdomen off the platform; score 4: arching of the body and lifting of the pelvic structures and scrotum.

2.4. Receptor functional study

2.4.1. Effect of DM506, TBG, and IBG at the 5-HT_{2A} receptor

The pharmacological activity of DM506, IBG, and TBG was assessed at the 5-HT_{2A} receptor as previously described [16]. The Homogeneous Time-Resolved Fluorescence (HTRF) IP-One G_q Detection kit was used to determine the accumulation of inositol monophosphate 1 (IP1) after receptor activation, according to the manufacturer's protocol. NIH/3T3 cells stably transfected with the 5-HT_{2A} receptor were seeded at a density of 3000 cells/well in 384-well plates in Opti-MEM medium. Then, test compounds were added, and the plates were incubated for 90 min at 37 °C, followed by 60 min incubation with Anti-IP1-Cryptate and IP1-d2 (IP-One G_q kit) at room temperature (RT). Stimulated IP-1 formation was determined *via* HTRF measurement.

2.4.2. Effect of DM506, TBG, and IBG at the 5-HT_6 receptor

The effects of DM506, TBG, and IBG on 5-HT_6 receptor-operated cAMP signaling were assessed in NG108–15 cells transiently expressing this receptor subtype, using the Bioluminescence Resonance Energy Transfer (BRET) sensor for cAMP, CAMYEL (i.e., cAMP sensor using YFP-Epac-RLuc) [34]. This cellular model allows for the assessment of drug effects on both 5-HT_6 receptor constitutive activity and agonist-stimulated activity at the G_s-adenylyl cyclase pathway [35]. Cells were co-transfected in suspension with constructs encoding the 5-HT_6 receptor and CAMYEL, using Lipofectamine 2000, according to the manufacturer's protocol, and grown in white 96-well plates at a density of 80,000 cells/well. Twenty-four hours after transfection, cells were washed with PBS containing calcium and magnesium and were exposed to compounds for 5 min in the same medium. Coelanterazine H was added at a final concentration of 5 μM and left at RT for 5 min. BRET was measured using a Mithras LB 940 plate reader (Berthold Technologies; Bad Wildbad, Germany).

2.4.3. Effect of DM506, TBG, and IBG at the 5-HT_7 receptor

Murine neuroblastoma N1E-115 cells were cultured in DMEM supplemented with 10 % FBS and 1 % penicillin/streptomycin. For cAMP measurement, a FRET-based biosensor was used, which shows a decreased FRET efficiency between mCerulean and Citrine upon increasing levels of cAMP [36]. Time-series measurements of cAMP dynamics were performed as previously described [37]. Briefly, N1E-115 cells were seeded onto 18 mm-coverslips and transfected with the 5-HT_7 receptor-mCherry and cAMP-biosensor constructs using Lipofectamine 2000 according to the manufacturer's protocol. On the day of experiment, cells were transferred to an osmolality-adjusted Tyrode

buffer (15 mM NaCl, 1 mM KCl, 0.1 mM $MgCl_2$, 0.2 mM $CaCl_2$, 1 mM HEPES, pH 7.4, D-glucose for osmolality adjustment). A Zeiss LSM780 (Oberkochen, Germany) equipped with a 40x/1.2 NA water immersion objective and the ZEN 2012 software was used for image acquisition. Imaging settings included a bit depth of 16 bit at 512×512 pixels. Citrine and mCerulean were excited at 440 nm and mCherry at 561 nm and spectra were unmixed using the "Online Fingerprinting Mode" of the ZEN 2012 software. To measure dynamic cAMP changes, images were captured every 10 s for 8 min with continuous focus correction using the Zeiss' "Definite Focus". The first three minutes were used to equilibrate the system. DM506, TBG, IBG, and 5-CT (a known agonist; [37]) were diluted at 10 μM in Tyrode buffer and were applied to the cells using a continuous perfusion system (Warner Instruments, Hollis-ton, MA, USA). To test inverse agonism, each ibogalogs and SB-269970 (10 μM) (a known inverse agonist; [37]) were administered two hours prior to the measurements and the phosphodiesterase inhibitor IBMX was applied at 50 μM at the indicated time points. For evaluation, ratio-time curves were calculated on a single-cell basis, after shift-correction and Gaussian blurring. The obtained curves were fitted to a single-exponential fit model, which provides the response amplitudes and response times. The calculated response amplitudes are reported as negative amplitudes, which correlate with the accumulation of cAMP. All computations were carried out using custom-written MATLAB scripts.

2.5. Statistical analysis of data

Statistical analyses were performed using Prism (GraphPad 10.0.3., La Jolla, CA, USA) and Origin 9 software (OriginLab, Northampton, MA, USA). Behavioral experiments were conducted by researchers blinded to the treatments. Behavioral results were analyzed by One-way ANOVA and post hoc Bonferroni's multiple comparisons test. Treatment of compounds was compared to vehicle treatment by One-way ANOVA with Dunnett's multiple comparison test. Values of $p \leq 0.05$ were considered statistically significant.

3. Results

3.1. Toxicity evaluation of DM506, TBG and IBG in mice

Before proceeding with the behavioral studies, we first investigated possible toxicity evoked by the acute administration of TBG (40 and 80 mg/kg), IBG (3 and 15 mg/kg), or DM506 (15 and 40 mg/kg). Following drug administration, behavioral, autonomic, and neurological parameters were evaluated in mice ($n = 4$) using the arbitrary score in the Irwin test [27] (Table 1). All ibogalogs at the highest doses induced behavioral alterations, in particular a decrease of spontaneous activity, reactivity, and curiosity, suggesting a calming effect. This correlates with the sedative effect observed with 40 mg/kg DM506 in mice [16]. In addition, TBG (80 mg/kg) and IBG (15 mg/kg), but not DM506 (40 mg/kg), reduced the palpebral opening of the mouse and increased its body temperature, leading to flushing of the anterior and posterior paws. Few minutes after TBG (80 mg/kg) or IBG (15 mg/kg) injection, mice developed tremors that lasted for about 30 min. However, tremorgenic activity was not observed at 3–10 mg/kg IBG, 40 mg/kg TBG, or 15–40 mg/kg DM506. Based on these results, the highest doses of IBG (15 mg/kg), TBG (80 mg/kg), and DM506 (40 mg/kg) were not used in the following behavioral studies. DM506 was the ibogalog with less potential to induce toxicological effects, even at high doses.

3.2. Effect of DM506, TBG, and IBG in the Chronic Constriction Injury (CCI) pain model

The effect of ibogalogs was challenged using a neuropathic pain model evoked by loose ligation of the sciatic nerve (i.e., CCI). To assess whether CCI induces hyperalgesia after a noxious mechanical stimulus (Paw pressure test) and/or allodynia after a non-noxious mechanical stimulus (von Frey test), both withdrawal latency and withdrawal threshold were respectively determined in the ipsilateral paw and compared to that in sham (control) animals eight days after the surgery. One-way ANOVA followed by Bonferroni post hoc comparison analysis of the paw pressure test (Fig. 2A,C,E) and von Frey test (Fig. 2B,D,F) results showed significantly reduced withdrawal values in CCI-treated animals compared to that in sham animals during the whole recording time ($p < 0.01$). These results indicated that CCI induces both mechanical hyperalgesia and allodynia in mice as previously observed [28].

Additional statistical analysis showed that ibogalogs, acutely administered, have a pain-relieving profile against both mechanical hyperalgesia and allodynia in mice, and in most cases these effects are dose- and timeframe-dependent. More specifically, analysis of the Paw pressure test results showed that DM506 acutely injected at a dose of 15 mg/kg, but not 5 mg/kg, significantly decreases mechanical hyperalgesia induced by sciatic nerve ligation at 15 min ($p < 0.05$), with a peak activity at 30 min ($p < 0.01$). This effect was still observed at 45 min although at a lower extent ($p < 0.05$), but then disappeared at 60–90 min ($p > 0.05$). A similar profile was observed using a non-noxious stimulus (i.e., von Frey test). DM506 (15 mg/kg) improved the withdrawal threshold (grams) at the ipsilateral paw in a dose-dependent manner (Fig. 2B). The peak of the anti-hypersensitivity effect was recorded at 30 min ($p < 0.01$), which was maintained until 60 min ($p < 0.01$) at a lower extent but was no longer effective at 90 min ($p > 0.05$). TBG administration also improved the mouse's withdrawal latency in a dose-dependent manner, compared to CCI + vehicle-treated animals (Fig. 2C). Following TBG (40 mg/kg) treatment, a significant decrease in the hyperalgesic activity was observed at 30 min ($p < 0.05$), with a peak recorded at 60 min ($p < 0.01$), which disappeared at longer times. A lower dose of TBG (15 mg/kg) showed a small, but significant effect only at 15 min ($p < 0.05$). TBG (15 and 40 mg/kg) was comparatively less effective against mechanical allodynia (i.e., von Frey test), slightly improving the paw withdrawal threshold at 30 min ($p < 0.05$ at both doses), with no dose-response effect (Fig. 2D). Since IBG has the narrowest therapeutic window based on the Irwin test results (Table 1), it was evaluated at only one low dose of 3 mg/kg (Fig. 2E,F). IBG was effective against mechanical hyperalgesia, significantly increasing the withdrawal latency of the ipsilateral paw between 15 and 90 min after treatment ($p < 0.01$), with maximal effect at 60 min ($p < 0.01$), whereas 24 h later the effect disappeared ($p > 0.05$) (Fig. 2E). Against mechanical allodynia, IBG significantly improved the withdrawal threshold at 60 min ($p < 0.01$) (Fig. 2F).

These results showed that ibogalogs decrease both mechanical hyperalgesia and allodynia. Since DM506, TBG and IBG did not improve the values reached on the contralateral (i.e., uninjured) paws (Table 2), we inferred that these compounds do not possess analgesic activity.

3.3. Effect of DM506, TBG, and IBG in the visceral pain model

The acute anti-hypersensitivity effect of ibogalogs was also studied in mice using a visceral pain model. Visceral pain was evaluated at the peak of colitis (day 8) reached after five days of DSS intake followed by three days of washout. One-way ANOVA followed by Bonferroni post hoc analysis showed that DSS-treated animals score significantly higher abdominal responses to colorectal distension induced by increased volumes (CRD, 50–200 μL) compared to control animals at all volumes and at all time points evaluated (p values of <0.01 and <0.001) (Figs. 3 and 4). This supports the notion that DSS induces visceral hypersensitivity [38].

Additional statistical analysis showed that the acute injection of DM506 (Fig. 3) and IBG (Fig. 4) completely abolished visceral hypersensitivity induced by DSS. More specifically, DM506 (15 mg/kg) significantly reduced the abdominal response of the animals to CRD between 30 min (Fig. 3A) and 90 min (Fig. 3C) ($p < 0.001$), compared to

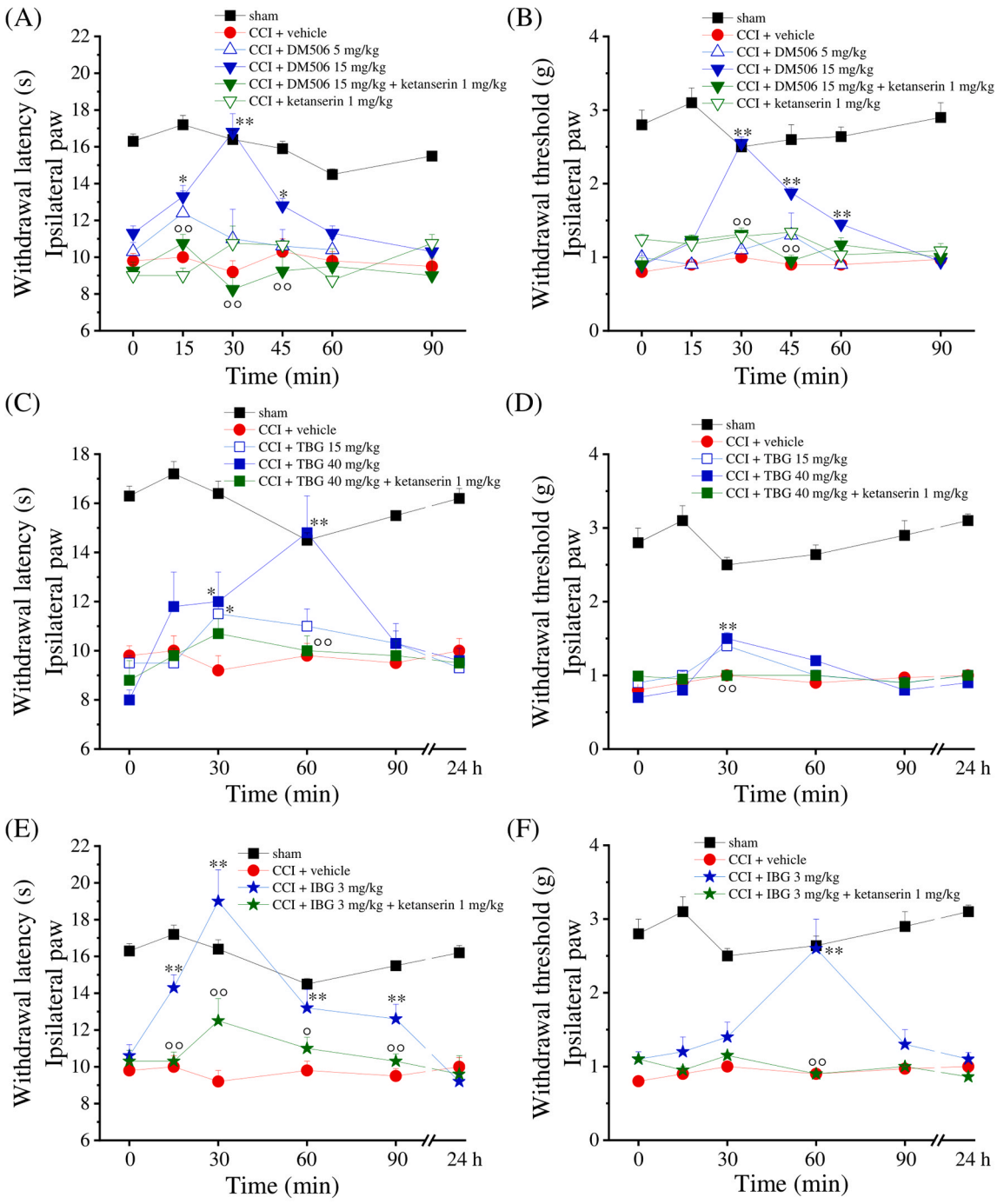

Fig. 2. Effect of acute administration of DM506, IBG, and TBG on CCI-induced neuropathic pain in mice. Ligation of the sciatic nerve was performed in mice (6–8 animals per group) to induce neuropathic pain. Surgery procedure but no sciatic nerve ligation was performed in sham (control) animals (■). Eight days after surgery, mice were injected (i.p.) 5 mg/kg (△) or 15 mg/kg (▼) DM506 (A,B), 15 mg/kg (□) or 40 mg/kg (■) TBG (C,D), and 3 mg/kg IBG (★) (C,D), or vehicle (●), and the response to a noxious (Paw pressure test) (A,C,E) and non-noxious (von Frey test) mechanical stimuli (B,D,F) was subsequently assessed on the ipsilateral paw. To determine the role of the 5-HT_{2A} receptor, ketanserin (1 mg/kg) was injected (i.p.) 30 min before the highest used dose of DM506 (15 mg/kg) (▼) (A,B), TBG (40 mg/kg) (■) (C,D), and IBG (3 mg/kg) (✻) (E,F), respectively. Statistical analysis of the results (mean ± SEM; n = 6–8 animals) showed that CCI + vehicle (●) decreased pain threshold in the paw pressure test (A,C,E) and von Frey test (B,D,F) [p <0.01 vs. sham animals (■) in both tests], respectively. (A,C,E) Statistical analysis of the paw pressure test results showed that 15 mg/kg (▼) (*p <0.05 at 15 and 45 min; **p <0.01 at 30 min), but not 5 mg/kg, DM506 (△) (A), 15 mg/kg (□) (*p <0.05 at 30 min) and 40 mg/kg (■) TBG (*p <0.05 at 30 min; **p <0.01 at 60 min) (C), and 3 mg/kg IBG (★) (**p <0.01 at 15–90 min) (E) significantly improved withdrawal latency compared to CCI + vehicle groups (●). The statistical analysis also showed that ketanserin significantly decreased the anti-neuropathic effect observed for DM506 (▼) (°°p <0.01 at 15, 30, and 45 min) (A), TBG (■) (°°p <0.01 at 60 min), and IBG (✻) (°°p <0.01 at 15, 30, and 90 min; °p <0.05 at 60 min), compared to the respective ibogalog-treated mice, without inducing any effect *per se* (△), compared to the CCI + vehicle group (●) (A). (B,D,F) Statistical analysis of the von Frey test results showed that 15 mg/kg (▼) (**p <0.01 at 30–60 min), but not 5 mg/kg (△), DM506 (B), 15 (□) and 40 mg/kg TBG (■) (*p <0.05 at 30 min for both doses) (D), and 3 mg/kg IBG (★) (**p <0.01 at 60 min) (F) significantly improved withdrawal threshold, compared to CCI + vehicle group (●). The statistical analysis also showed that ketanserin significantly decreased the anti-neuropathic effect observed for DM506 (▼) (°°p <0.01 at 30 and 45 min) (B), TBG (■) (°°p <0.01 at 30 min) (D), and IBG (★) (°°p <0.01 at 60 min) (F), compared to the respective ibogalog-treated mice, without inducing any effect *per se* (▽), compared to the CCI + vehicle group (●) (B).

Table 2
Effect of acute administration of DM506, TBG, and IBG in the contralateral paw of the mouse using the CCI model.

Time	Sham	CCI + vehicle	CCI + DM506	CCI + TBG	CCI + IBG
	Withdrawal latency (s) in the contralateral paw[a]				
Pretest (0 min)	17.0 ± 0.6	17.7 ± 0.7	17.3 ± 1.1	17.8 ± 1.1	17.2 ± 0.5
15 min	16.3 ± 0.6	17.0 ± 0.9	17.5 ± 1.3	18.7 ± 0.8	18.3 ± 1.9
30 min	17.3 ± 0.8	16.0 ± 0.8	18.5 ± 0.4	17.5 ± 1.0	18.8 ± 1.1
45 min	18.9 ± 1.3	16.3 ± 0.9	15.0 ± 0.5	not determined	not determined
60 min	17.7 ± 0.8	17.0 ± 1.0	16.5 ± 0.7	16.3 ± 0.6	14.8 ± 0.5
90 min	17.5 ± 1.0	17.3 ± 1.3	16.3 ± 0.8	16.3 ± 0.4	16.8 ± 0.5
24 h	18.2 ± 0.5	16.0 ± 1.1	not determined	17.0 ± 0.8	15.8 ± 0.6
Time	Withdrawal threshold (g) in the contralateral paw[b]				
Pretest (0 min)	2.3 ± 0.1	2.8 ± 0.2	2.2 ± 0.1	2.7 ± 0.6	2.7 ± 0.2
15 min	2.5 ± 0.1	2.7 ± 0.1	2.5 ± 0.2	2.8 ± 0.2	2.3 ± 0.07
30 min	2.6 ± 0.08	3.1 ± 0.2	2.8 ± 0.1	3.0 ± 0.3	2.8 ± 0.3
45 min	2.5 ± 0.07	2.4 ± 0.1	2.5 ± 0.2	not determined	not determined
60 min	2.8 ± 0.1	2.6 ± 0.1	2.6 ± 0.1	2.8 ± 0.07	2.6 ± 0.2
90 min	2.8 ± 0.1	2.8 ± 0.2	2.2 ± 0.08	2.6 ± 0.1	2.5 ± 0.3
24 h	2.6 ± 0.1	2.9 ± 0.1	not determined	2.7 ± 0.2	3.0 ± 0.2

Ligation of the sciatic nerve was performed in mice (6–8 animals per group) to induce neuropathic pain. Surgery procedure but no sciatic nerve ligation was performed in sham (control) animals. Eight days after surgery, mice were injected (i.p.) with 15 mg/kg DM506, 40 mg/kg TBG, 3 mg/kg IBG, or vehicle. The response to a noxious[a] or non-noxious[b] mechanical stimuli was subsequently assessed in the contralateral paw of the mouse using the Paw pressure test[a] and von Frey test[b], respectively. Data are expressed as mean ± SEM.

DSS-treated animals. Interestingly, DM506 was still active at 240 min when animals were subjected to 50 μL ($p < 0.01$) or 100 μL ($p < 0.05$) CRD (Fig. 3D) although with lower efficacy in comparison to that recorded at 30–90 min.

IBG (3 mg/kg) (Fig. 4A-C) and TBG (40 mg/kg) (Fig. 4D,E) were also effective in relieving DSS-induced visceral pain despite differences in efficacy. Statistical comparisons with DSS-treated animals, showed that IBG significantly reduced the AWR score at 30 min to a colorectal distension caused by 100–200 μL (Fig. 4A) and at 60 min caused by a volume of 150 μL ($p < 0.01$ at both times) (Fig. 4B), which disappeared at 90 min ($p > 0.05$) (Fig. 4C). TBG showed a short-term and a lower effect since the activity was observed 30 min after a colorectal distension caused by 100–200 μL ($p < 0.05$) (Fig. 4D), but not at 60 min ($p > 0.05$) (Fig. 4E).

3.4. The anti-pain activity of TBG, IBG, and DM506 was reverted by ketanserin

We also investigated whether the 5-HT_{2A} receptor is involved in the observed activity of ibogalogs on both CCI and DSS mouse models. In this regard, ketanserin (1 mg/kg), a potent 5-HT_{2A} receptor antagonist [22–24], was injected (i.p.) 30 min before ibogalog administration at their highest doses. Statistical analysis of the results showed that ketanserin completely blocks the pain-relieving effect of 15 mg/kg DM506 ($p < 0.01$ at all times) (Fig. 2A,B), 40 mg/kg TBG ($p < 0.01$ at all times) (Fig. 2C,D), and 3 mg/kg IBG ($p < 0.01$ at 15, 30, and 90 min; $p < 0.05$ at 60 min) (Fig. 2E,F), respectively, compared to ibogalog-treated mice. Ketanserin *per se* does not affect the animal's pain threshold, as no difference was found in comparing CCI-treated animals they received ketanserin 1 mg/kg or vehicle (Fig. 2A,B).

Statistical analysis of the DSS results demonstrated that ketanserin blocks the pain-relieving effect of 15 mg/kg DM506 ($p < 0.01$) at 30 min at all volumes used for the colorectal distension (Fig. 3A). At the other time points evaluated, ketanserin was no longer effective (Fig. 3B,C,D). Notably, ketanserin *per se* did not affect pain sensitivity in the DSS mouse model ($p > 0.05$) (Fig. 3A,B). Moreover, ketanserin completely blocked the pain-relieving activity of 3 mg/kg IBG at 30 min ($p < 0.01$ at 100–150 μL) (Fig. 4A,B). TBG was not investigated since it was barely effective against this kind of pain.

3.5. DM506, IBG, and TBG activate the 5-HT_{2A} receptor

Functional experiments were performed to determine the activity of DM506, IBG, and TBG at the 5-HT_{2A} receptor (Fig. 5). The results showed that all compounds act as potent agonists of this receptor subtype, with potency sequence as follows: DM506 (9.0 ± 3.5 nM) > IBG (28 ± 10 nM) > TBG (197 ± 43 nM) (Table 3). Considering 100 % efficacy (E_{max}) for 5-HT, we can conclude that TBG (91 ± 18 %) and IBG (93 ± 16 %) reached E_{max} values corresponding to full agonists of the 5-HT_{2A} receptor, whereas DM506 (76 ± 16 %) behaved as a partial agonist (Table 3).

3.6. DM506, TBG, and IBG activate the 5-HT_6 receptor

In line with the role of 5-HT_6 receptor constitutive activity in painful symptoms observed in several neuropathic pain paradigms [11–13], we explored possible agonist/inverse agonist effects of DM506, TBG, and IBG in NG108–15 cells transiently expressing recombinant 5-HT_6 receptors, a cellular model that allows for the assessment of drug effects on 5-HT_6 receptor constitutive activity at the G_s-adenylyl cyclase pathway in addition to agonist-stimulated activity (Fig. 6). WAY181187 [39] and intepirdine [40] were used as reference agonist and inverse agonist, respectively. In contrast to intepirdine, which inhibited constitutive activation of cAMP production (IC_{50} = 5.7 ± 2.1 nM), DM506 (EC_{50} = 2.9 ± 0.9 nM) and IBG (EC_{50} = 7.1 ± 2.2 nM) concentration-dependently increased cAMP production in NG108–15 cells with similar potencies (Table 3) as that measured for WAY181187 (EC_{50} = 3.2 ± 0.3 nM). The E_{max} values indicated that both ibogalogs are potent, full agonists of the 5-HT_6 receptor when compared to the full agonist WAY181187 (Table 3). Although TBG was as efficient as WAY181187 to stimulate cAMP production in NG108–15 cells, it exhibited a lower potency (EC_{50} = 132 ± 38 nM).

3.7. DM506 and IBG, but not TBG, behave as inverse agonists of the 5-HT_7 receptor

It has been previously demonstrated that IBG acts as an inverse agonist of the 5-HT_7 receptor [14]. Therefore, we next investigated whether IBG, TBG, and DM506 can modulate 5-HT_7 receptor-mediated signaling. To this end, mCherry-tagged 5-HT_7 receptor was co-expressed with the FRET-based cAMP biosensor CEPAC [36] (Fig. 7A). This biosensor includes the cAMP-binding domain of the EPAC protein cloned between mCerulean (FRET donor) and Citrine (FRET acceptor). Upon cAMP binding, conformational changes of the sensor occur, leading to a decrease in the FRET signal (Fig. 7B). The cAMP responses were recorded at the single-cell level by monitoring the CEPAC fluorescence intensity ratio of the acceptor to the donor (A/D ratio). The strength of receptor-mediated signaling was determined from the amplitude of the CEPAC fluorescence intensity ratio.

First, we tested whether TBG, IBG, and DM506 possess agonistic properties toward the 5-HT_7 receptor. In these experiments, 5-CT, a specific 5-HT_7 receptor agonist [37], was used as a positive control. As shown in Figs. 7C and 7D, treatment of 5-HT_7 receptor expressing cells with 10 μM 5-CT resulted in a decrease in the A/D ratio of the biosensor

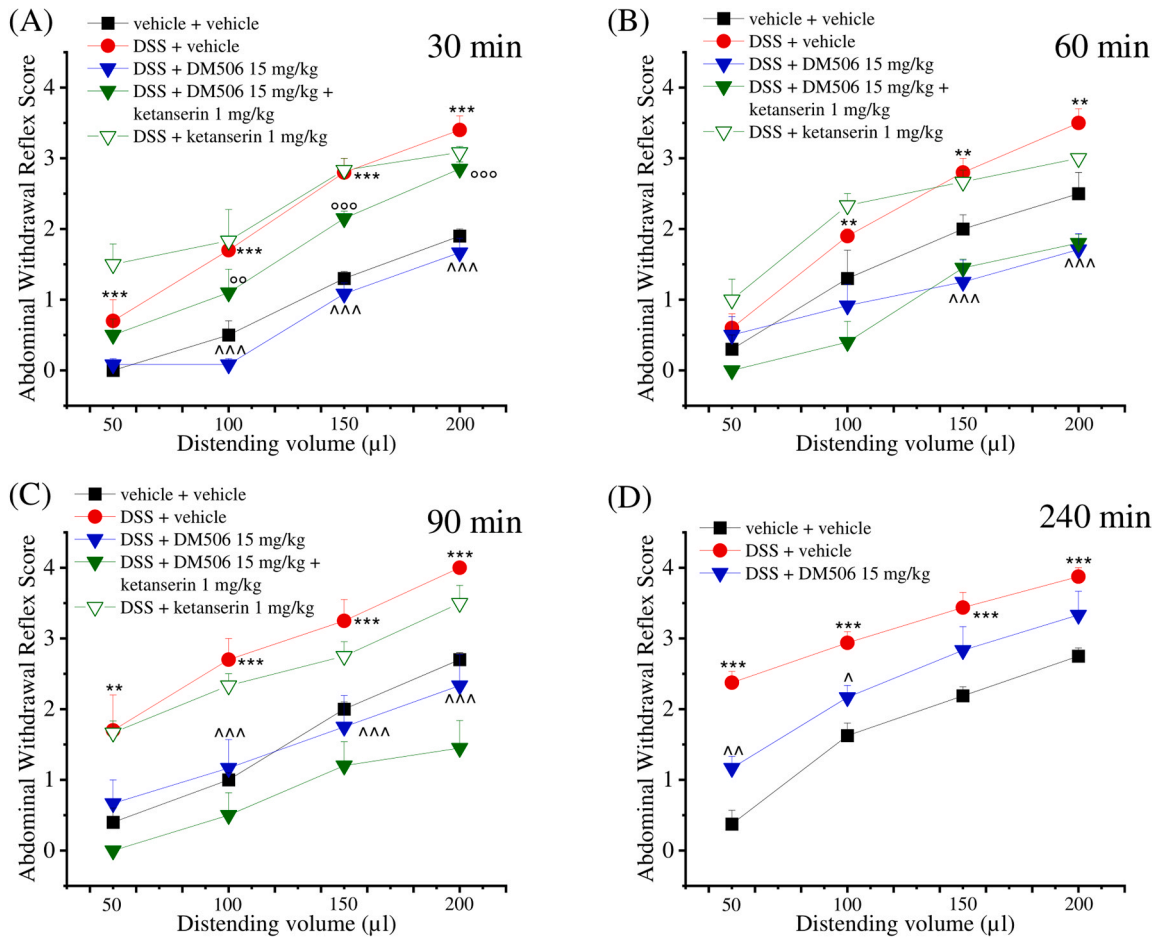

Fig. 3. Effect of acute administration of DM506 on DSS-induced visceral pain in mice. Animals were treated with DSS (●), or vehicle (■), for 5 consecutive days to induce hyperalgesic pain. On day 8, mice were administered (i.p.) 15 mg/kg DM506 (▼), or vehicle (■). Visceral sensitivity was assessed by measuring the extent of the abdominal withdrawal response (AWR) to colorectal distension induced by increased volumes (50–200 µL) at 30 (A), 60 (B), 90 (C), and 240 min (D), respectively. To determine the role of the 5-HT_{2A} receptor, ketanserin (1 mg/kg) was injected (i.p.) 30 min before DM506 (15 mg/kg) (▼), or vehicle (A,B,C). Each value represents the mean ± SEM of 6–8 animals per group performed in two different experimental sets. Statistical analysis of the results showed that DSS induces visceral pain in the 30–240 min time regime (**p <0.01 and ***p < 0.001 *vs* vehicle + vehicle), and that DM506 (▼) significantly decreased DSS-induced visceral pain at 30 min (^^^p <0.001 at 100–200 µL), 60 min (^^^p <0.001 at 150–200 µL), 90 min (^^^p <0.001 at 100–200 µL), and 240 min (^p <0.01 at 50 µL; ^p <0.05 at 100 µL), compared to DSS + vehicle-treated animals (●). The statistical analysis also showed that ketanserin (▼) significantly decreased the anti-hypersensitivity effect observed for DM506 at 30 min (°°p <0.01), but not at 60–90 min (p >0.05), with respect to ibogalog-treated mice, without inducing any effect *per se* (▽), compared to DSS-treated group (●).

indicating cAMP production. In contrast, application of either 10 µM TBG, IBG, or DM506 did not result in any changes of [cAMP] (Fig. 7C,D). One-way ANOVA and Dunnett's ad hoc analysis of the results showed that the maximal response for 5-CT (27.0 ± 9.6 %) was significantly higher (p <0.001) than that for vehicle (2.9 ± 4.5 %), which in turn was similar as that for DM506 (2.7 ± 2.4 %), IBG (0.6 ± 0.9 %), and TBG (3.6 ± 0.4 %), respectively (p >0.05), demonstrating that these ibogalogs are not 5-HT_7 receptor agonists.

We next analyzed whether the presence of ibogalogs can modulate constitutive activity of 5-HT_7 receptor by measuring the accumulated cAMP after blocking cAMP degradation by the phosphodiesterase inhibitor IBMX (50 µM). As shown in Fig. 7E-G, the cAMP biosensor ratio decreased after the application of IBMX in cells expressing either 5-HT_7 receptor, confirming its high constitutive activity. Simultaneous application of IMBX and 10 µM SB-269970, a highly selective inverse agonist of the 5-HT_7 receptor [37], blocked the accumulation of cAMP. Similar results were obtained after co-application of IMBX with either IBG or DM506, while TBG did not result in any significant effect (Fig. 7E-G). Statistical analysis of the results showed that the maximal IBMX (i.e., IBMX+vehicle) response was significantly blocked by SB-269970 (56.1 ± 6.5 %; p <0.0001), DM506 (52.3 ± 12.7 %; p <0.001), and IBG (35.9 ± 10.0 %; p <0.01), but not by TBG (14.3 ± 11.9 %; p >0.05) (Table 3). These results demonstrated that DM506 and IBG, but not TBG, behave as inverse agonists of the 5-HT_7 receptor.

4. Discussion

The primary objective of this study was to determine in mice the activity of DM506, TBG, and IBG against two different types of pain, visceral and neuropathic pain [19,20]. To determine potential molecular mechanisms, the role of the 5-HT_{2A}, 5-HT_6, and/or 5-HT_7 receptor was assessed using behavioral and functional approaches.

The CCI study showed that DM506, TBG, and IBG decrease mouse neuropathic pain induced by sciatic nerve ligation in a dose- and timeframe-dependent manner, with no observable toxicological effects. The paw pressure test results showed that ibogalogs have anti-hyperalgesic activity against a noxious stimulus. More specifically, DM506 (15 mg/kg) induced maximal activity (30 min) earlier than TBG (40 mg/kg) or IBG (3 mg/kg) (60 min). A lower dose of IBG showed the longest effect (90 min) compared to DM506 (45 min) and TBG (60 min), respectively. Ibogalogs also decreased mechanical allodynia (i.e., von

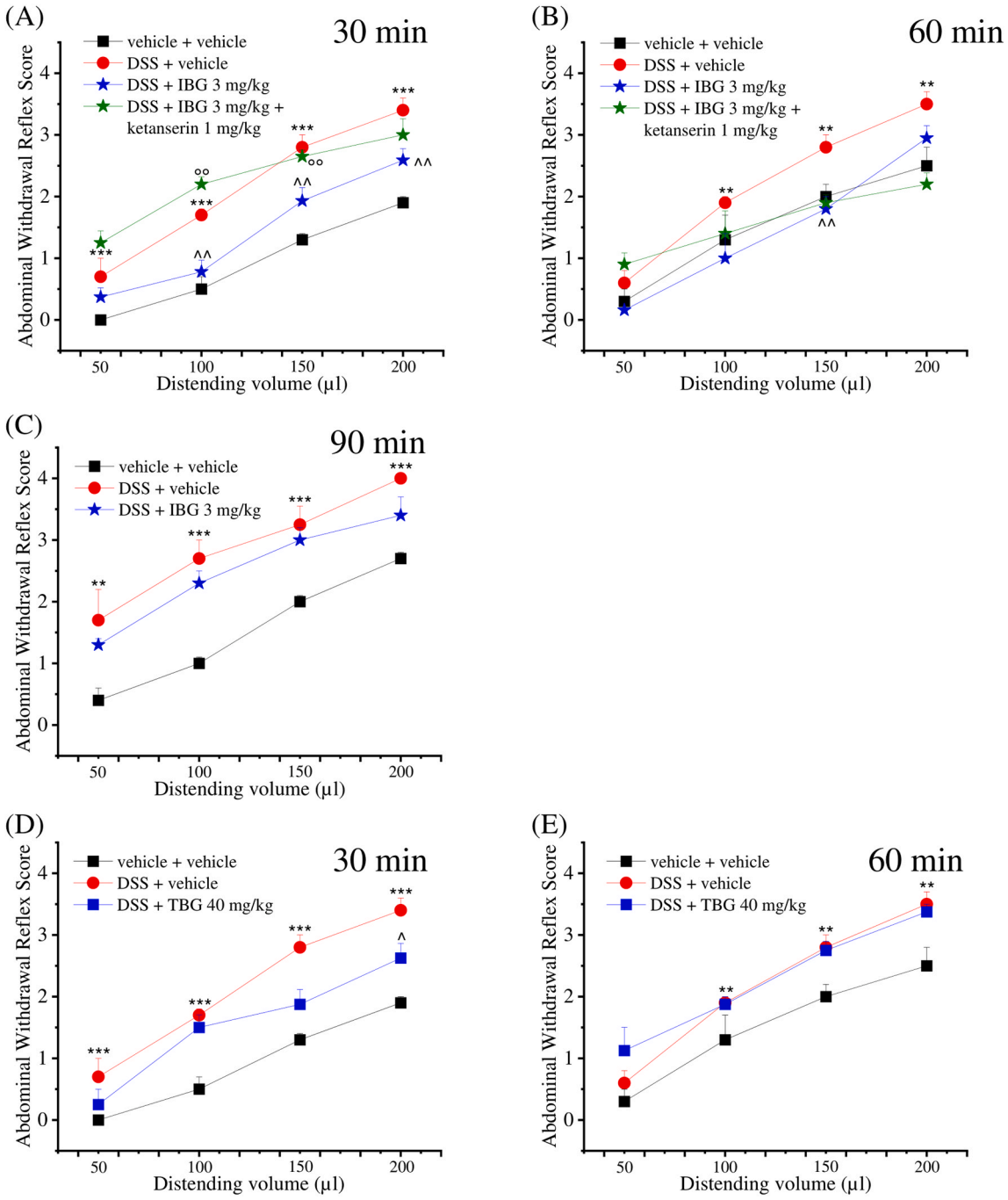

Fig. 4. Effect of the acute administration of IBG and TBG on DSS-induced visceral pain in mice. Animals were treated with DSS (●), or vehicle (■), for 5 consecutive days to induce hyperalgesic pain. On day 8, mice were administered (i.p.) 3 mg/kg IBG (★) (A-C) or 40 mg/kg TBG (■) (D,E), or vehicle (■). Visceral sensitivity was assessed by measuring the extent of the AWR to colorectal distension (50–200 µL) at 30 min (A), 60 min (B), and 90 min (C) for IBG, and at 30 min (D) and 60 min (E) for TBG. To determine the role of the -5-HT_{2A} receptor, ketanserin (1 mg/kg) was injected (i.p.) 30 min before IBG (3 mg/kg) (★) (A,B). Each value represents the mean ± SEM of 6–8 animals per group performed in two different experimental sets. Statistical analysis of the results showed that DSS (●) induces visceral pain in the 30–90 min time regime (**p <0.01 and ***p <0.001 *vs* vehicle + vehicle), and that IBG (★) at 30 min (^^p <0.01 at 100–200 µL) (A) and 60 min (^^p <0.01 at 150 µL) (B), and TBG (■) at 30 min (^p <0.05 at 200 µL) (D) significantly improve visceral pain, compared to DSS + vehicle-treated animals (●). Ketanserin completely counteracted the anti-hypersensitivity effect observed for IBG (★) at 30 min (°°p <0.01 at 100–150 µL) in comparison to the respective ibogalog-treated mice.

Frey test) with a similar profile as that observed in the Paw pressure test. The observed differences among compounds might simply be the result of variations in pharmacokinetics and/or metabolic processes. These results clearly demonstrated that ibogalogs decrease both mechanical hyperalgesia and allodynia, two conditions usually observed in neuropathic pain [41]. Considering that ibogalogs did not induce analgesic effect as highlighted in this work, we can discard a mechanism involving activation of opioid receptors, which coincides with the lack of pharmacological activity at these receptors [14].

Our study also showed that DM506, TBG, and IBG completely abolish visceral pain in mice. Although all ibogalogs reduced the abdominal response to different colorectal distension volumes, the observed reduction of visceral hypersensitivity was different among compounds. More specifically, DM506 showed the longest effect (up to 240 min), up

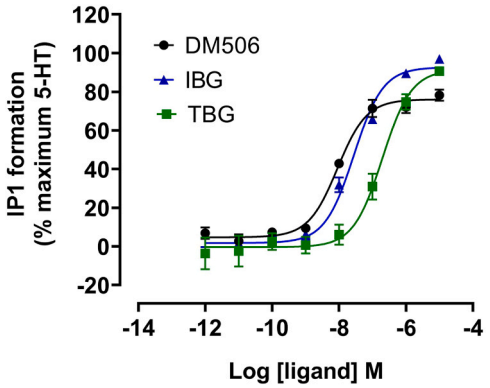

Fig. 5. Functional activity of DM506, IBG, and TBG at the human 5-HT_{2A} receptor. NIH/3T3 cells expressing this receptor subtype were incubated (90 min) with different concentrations of DM506 (●), IBG (▲), or TBG (■). Activation of the 5-HT_{2A} receptor was assessed by IP1 formation. Receptor activation data were normalized considering 0 % as the baseline signal and 100 % as the maximum 5-HT-stimulated signal. Data are shown as mean ± SEM from at least three experiments, each performed in triplicate. The calculated EC_{50} and E_{max} values are summarized in Table 3.

Table 3
Pharmacological activity of ibogalogs at different 5-HT receptor subtypes.

Receptor Subtype	Compound	EC_{50} (nM)	E_{max} (%)	Inhibition of maximal response (%)
5-HT_{2A}[a]	DM506	9.0 ± 3.5	76 ± 16	–
	TBG	197 ± 43	91 ± 18	–
	IBG	28 ± 10	93 ± 16	–
5-HT_6[b]	DM506	2.9 ± 0.9	96 ± 4	–
	TBG	132 ± 38	133 ± 8	–
	IBG	7.1 ± 2.2	99 ± 5	–
5-HT_7	DM506	–	–	52.3 ± 12.7[c]
	IBG	–	–	35.9 ± 10.0[c]
	TBG	–	–	14.3 ± 11.9[c]

EC_{50}, activation potency
E_{max} (efficacy) percentages were obtained considering 100 % activation by 5-HT[a] or WAY181,187[b].
[a] Data for DM506 (taken from [16]) were included for comparative purposes.
[b] Data for the 5-HT_6 receptor subtype were calculated from Fig. 6.
[c] Inhibition of maximal IBMX+vehicle response (%) obtained at 10 μM ibogalog (taken from Fig. 7G).

to a distension volume of 150 μL), whereas IBG presented a medium-lasting effect (30–60 min), and TBG displayed the shortest and least effect (only at 30 min). This behavioral profile was different to that observed using the CCI model, where IBG showed the most potent and long-lasting anti-hyperalgesic and anti-allodynic activity. This might be due to differences in ligand selectivity and potency at a variety of receptors expressed in neuronal pathways involved in distinct pain conditions. To this respect, the 5-HT_{2A} receptor is highly expressed in the myenteric and submucosal neurons of the gastro-intestinal tract, playing roles in various enteric functions, including contraction of the smooth muscle [42]. Thus, it is plausible that the decreased visceral pain observed with ibogalogs is mediated by enteric 5-HT_{2A} receptors but not 5-HT_{2C} receptors, which are less expressed in the enteric nervous system [43]. On the other hand, Okamura and colleagues demonstrated that intracisternal injection of ketanserin blocked levodopa-induced visceral antinociception, indicating that the brain 5-HT_{2A} receptor plays an important role, supporting the implication of gut-brain axis in the

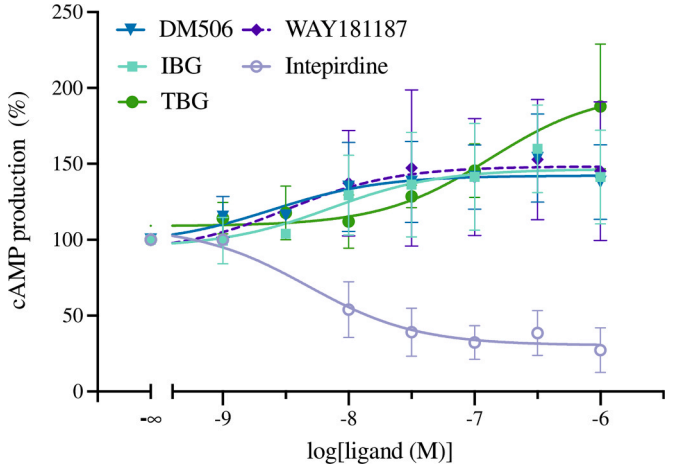

Fig. 6. Effect of DM506, TBG, IBG, WAY181187, and intepirdine on 5-HT_6 receptor-mediated cAMP signaling. Neuroblastoma NG108–15 cells transiently transfected with plasmids encoding the 5-HT_6 receptor and the BRET cAMP sensor CAMYEL were exposed to increasing concentrations of DM506 (▲), IBG (■), TBG (●), WAY181187 (◆) (a known full agonist), or intepirdine (○) (a known inverse agonist), for 5 min. Each point represents the mean ± SEM of the BRET signals (expressed in % of values measured in vehicle-treated cells) obtained from quadruplicates measurements in five independent experiments performed on different sets of cultured cells. The EC_{50}, IC_{50}, and E_{max} values are summarized in Table 3.

pathophysiology of visceral pain [44].

In recent years, identifying the role of metabotropic 5-HT receptors in pain modulation is becoming a hot topic [45]. Whether the effect is to facilitate or inhibit pain transmission is strictly related to the receptor subtype and the sites of action [46,47]. The 5-HT_2 receptor subfamily consists of 5-HT_{2A}, 5-HT_{2B}, and 5-HT_{2C} subtypes. Although this receptor subfamily shows in general excitatory activity, the 5-HT_{2A} receptor, the most studied subtype in neuropathic pain models, also has inhibitory effects. The 5-HT_{2A} receptor is expressed in several brain areas such as nucleus raphe magnus and ventrolateral periaqueductal gray, which are part of the descending pain-modulation pathway (reviewed in [4]). To assess the involvement of the 5-HT_{2A} receptor in the anti-hypersensitivity activity of ibogalogs, we determined the effect of ketanserin [14,22–24] in the anti-neuropathic activity of DM506, TBG, and IBG. The results showed that ketanserin inhibits the anti-neuropathic activity of each compound. Despite ketanserin binds 5-HT_{2A} (K_i = 1.13 nM), 5-HT_{2B} (K_i = 234 nM), and 5-HT_{2C} (K_i = 88 nM) receptor subtypes, it has 207- and 78-fold higher affinity for the 5-HT_{2A} receptor subtype [23]. In this regard, we used a low dose of ketanserin (1 mg/kg) to increase the selectivity toward the 5-HT_{2A} receptor.

A recent study from our lab showed that DM506 [16], but neither TBG nor IBG [14], potently activates the 5-HT_{2B} receptor, discarding this receptor subtype as part of the behavioral activity elicited by the studied ibogalogs. Considering that TBG and IBG also behave as agonists of the 5-HT_{2C} receptor subtype [14], another possibility is that ibogalog's activity is partially mediated through this receptor subtype. Previous studies showed that 5-HT_{2C} receptor agonists (e.g., meta-chlorophenylpiperazine) induce anti-neuropathic activity in rats, which was reduced by a selective antagonist [7] (reviewed in [6]). However, 5-HT_{2C} receptor knockdown in the amygdala reduced neuropathic pain [48], indicating that the lack of 5-HT_{2C} receptor function, not its stimulation, is involved in this process.

In principle these results support the notion that ketanserin blocks the anti-neuropathic activity of ibogalogs *via* 5-HT_{2A} receptor inhibition. Proving this statement is the behavioral result with volinanserin, an antagonist with higher selectivity for the 5-HT_{2A} receptor than ketanserin [23,49], which inhibited the anti-neuropathic pain activity of DM506 in mice [50] with similar efficacy as that elicited by ketanserin

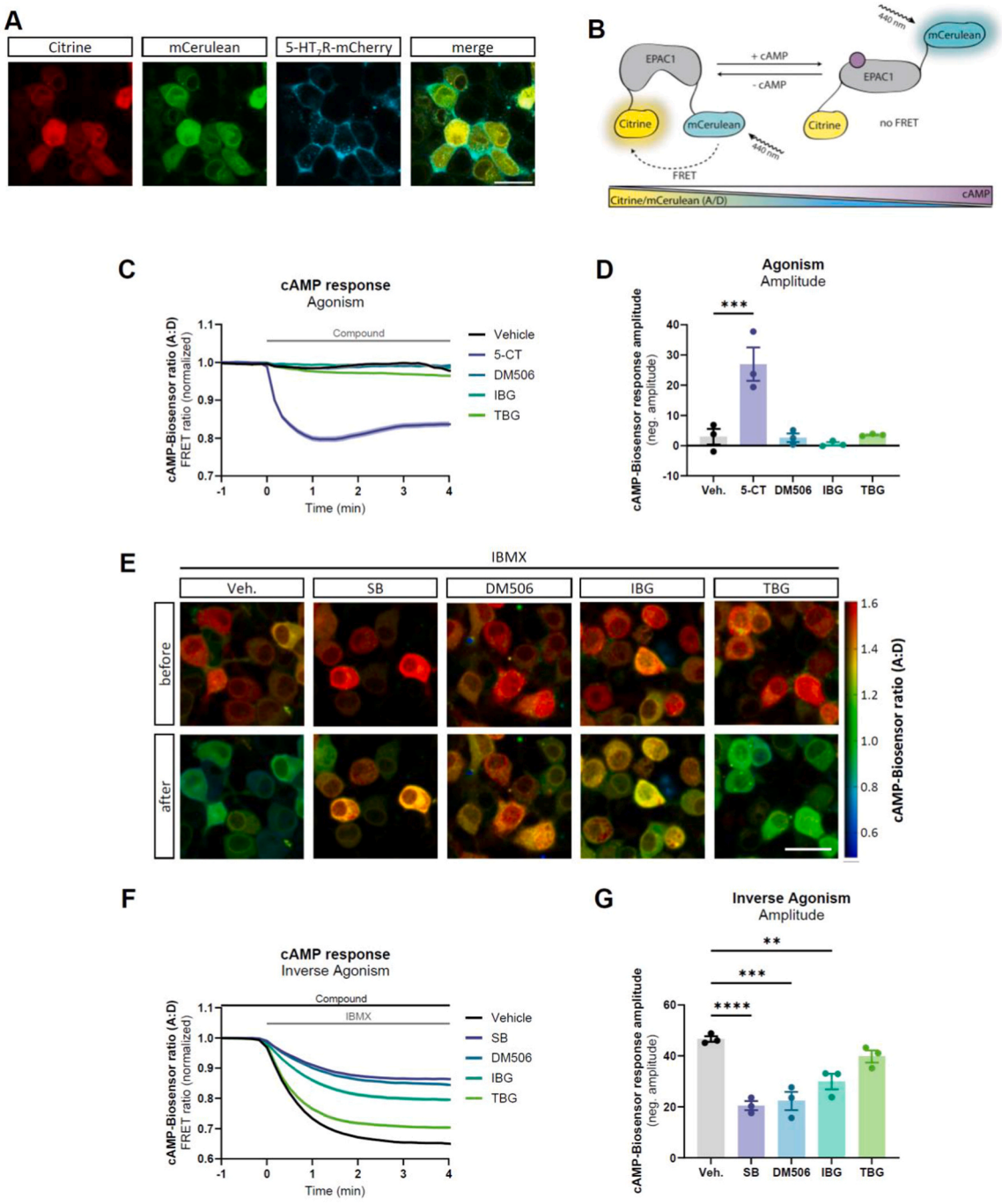

Fig. 7. Effect of ibogalogs on 5-HT$_7$ receptor-mediated cAMP signaling. (A) Representative images of N1E-115 cells expressing the cAMP biosensor and 5-HT$_7$ receptor-mCherry. Scale bar: 30 μm. (B) Schema of the FRET-based cAMP biosensor. With increasing levels of cAMP, the FRET efficiency as well as the Citrine/mCerulean (acceptor/donor, A/D) ratio decreases. (C) Response-time curves of the cAMP biosensor ratio in response to the treatment with 10 μM DM506, IBG, or TBG. Stimulation with vehicle (Veh) and 10 μM 5-CT were used as negative and positive control, respectively. (D) Response amplitudes were calculated from the respective response-time curves. (E-G) Inverse agonism was tested by the inhibition of 5-HT$_7$ receptor-mediated and IBMX-facilitated accumulation of cAMP. Cells were pre-treated with DM506, IBG, or TBG, and the cAMP biosensor ratio was measured in response to the application of 50 μM IBMX. Vehicle and 10 μM SB-269970 (SB) were used as negative and positive control, respectively. (E) Representative images of the cAMP biosensor ratio in N1E-115 cells before and after application of IBMX. Cells were pre-treated as indicated. Scale bar: 30 μm. (F) Response-time curves of the cAMP-biosensor ratio in response to IBMX. (G) Response amplitudes were calculated from the respective response-time curves and summarized in Table 3. Data are presented as mean ± SEM (n=3 independent experiments). **p <0.01; ***p <0.001; ****p <0.0001.

(this work). Since neither ketanserin (this work) nor volinanserin [50] changed the pain threshold *per se*, and DM506, TBG, and IBG behave as agonists of the 5-HT$_{2A}$ receptor [14,16; this work], we suggest that these compounds decrease neuropathic pain through a mechanism involving activation of the 5-HT$_{2A}$ receptor. These results support previous studies showing that the activation of the 5-HT$_2$ receptor in dorsal horn neurons induces anti-neuropathic activity but contradict the notion that 5-HT$_{2A}$ receptor antagonists decrease neuropathic pain (reviewed in [4,6]). On the other hand, there is evidence that ketanserin also inhibits histamine H1 and adrenergic α1 receptors [23]. Considering that TBG (10 μM) also

inhibited both α1 (~15–20 %) and H1 (~35 %) receptors [14], it is obvious that ketanserin cannot block ibogalog's effects, indicating that these receptor types are not involved in the anti-neuropathic activity of ibogalogs.

Studies in cell cultures expressing either the 5-HT_6 or 5-HT_7 receptor showed that TBG, IBG, and DM506 are potent agonists at the former receptor subtype but behave as inverse agonists (except TBG) at the latter. In general, these results supported a previous study using TBG and IBG [14]. Nevertheless, the activity of TBG at the 5-HT_7 receptor was distinct: it did not show agonistic or inverse agonistic activity. Considering that 5-HT_7 receptor activation induces antinociceptive and anti-inflammatory effects in rodents [8–10], we can rule out 5-HT_7 receptor inhibition as a plausible mechanism for the pain relieving activity of ibogalogs. Our results at the 5-HT_6 receptor also showed full agonistic activity for the three compounds, compared to the full agonist WAY181, 187 [39], whereas Cameron et al. [14] observed a partial agonistic activity for TBG (88 %) and IBG (83 %) compared to 5-HT. Considering that 5-HT_6 receptor inhibition mediated by inverse agonists induced anti-neuropathic effects in rodents [11–13], we can discard 5-HT_6 receptor activation as a potential mechanism for the pain-relieving effects of ibogalogs. Nevertheless, we cannot rule out that 5-HT_6 receptor activation might decrease symptoms of anxiety and depression [51] often observed in chronic pain [52]. An important methodological detail is that the activity of ibogalogs was determined using assays specifically designed to detect the functional properties of each receptor subtype. The 5-HT_{2A} receptor is canonically coupled to the G_q protein, while both 5-HT_6 and 5-HT_7 receptors are canonically coupled to G_s. This explains why we measured IP1 production to assess ibogalog-induced 5-HT_{2A} receptor activation and cAMP level to evaluate the effects of these compounds at both 5-HT_6 and 5-HT_7 receptors. To determine the effects of the compounds on the 5-HT_6 receptor, we used NG108–15 neuroblastoma cells, where the receptor exhibits a high level of constitutive activity at various signaling pathways, allowing the assessment of agonist, inverse agonist, or antagonist activity [35,53]. We also used neuroblastoma x glioma hybrid N1E-115 cells, which do not endogenously express any 5-HT receptor, allowing precise measuring activity of individual 5-HT receptors such as the 5-HT_7 receptor. This receptor was co-expressed with a FRET-based cAMP biosensor, which permits the measurement of response amplitudes to finally assess agonist or inverse agonist activity [37,54].

Our previous study on nAChRs showed that TBG, IBG, and DM506 inhibit the α9α10 nAChR subtypes with higher potencies than that for the voltage-gated N-type calcium channel ($Ca_V2.2$) [26,55], ruling out this channel as a target for the behavioral effects of ibogalogs. Although inhibition of the α9α10 nAChR expressed in immunocompetent cells has been considered an important mechanism for anti-inflammatory and anti-neuropathic effects [56,57], the inhibitory potency of TBG (IC_{50} = 4.8 μM), IBG (13.0 μM), and DM506 (5.1 μM) at the α9α10 nAChR [26,55] is much lower than that elicited at the 5-HT_{2A} receptor (this work), discarding the possibility that the anti-neuropathic and anti-allodynic activity of ibogalogs is mediated by α9α10 nAChR inhibition.

This work demonstrated, for the first time, that ibogalogs abolish neuropathic and visceral pain by decreasing mechanical allodynia and hyperalgesia, without inducing analgesic effects. Activation of the 5-HT_{2A}, but neither activation of the 5-$HT_{2\,C/2B}$ or 5-HT_6 receptor nor inhibition of the 5-HT_7 receptor, is an important initial step for the anti-neuropathic and anti-allodynic activity of ibogalogs. These results gave a better understanding of the function of various 5-HT receptor subtypes in the modulation of different types of pain and support the development of novel therapies for a variety of pain symptoms.

Author contributions

HRA developed the concept, wrote part of the introduction and discussion. LM performed the animal studies and wrote the results. CC performed the animal studies. DR performed the 5-HT_{2A} receptor study and wrote the results. OB performed the 5-HT_6 receptor study and wrote the results. EP and SB performed the 5-HT_7 receptor study and wrote the results. DM and MNR synthesized DM506. HRA, LM, EP, PM, DR, CG, MEL, and LDCM performed data analyses and contributed to critical comments on the discussion.

Funding

This work was supported by the Italian Ministry of Instruction, University and Research (MIUR), Italy (to CG and LDCM), from University of Florence, Italy (to MNR and DM), ANR (no ANR-19-CE18–0018–02 and ANR-22-CE92–0073–01) (to PM), the DFG grant PO732, AFI grant #21043, and Alzheimer's Association grant #1141447 (to EP), and by an OVPR Pilot/Seed Grant (Oklahoma State University Center for Health Sciences) (to HRA).

CRediT authorship contribution statement

Dina Manetti: Methodology, Investigation. **Maria Novella Romanelli:** Methodology, Investigation. **Evgeni Ponimaskin:** Writing – original draft, Supervision, Data curation. **Ophelie PhD Bento:** Formal analysis. **Saskia Borsdorf:** Investigation. **Clara Ciampi:** Investigation. **Philippe Marin:** Data curation. **Carla Ghelardini:** Funding acquisition. **Lorenzo Di Cesare Mannelli:** Writing – original draft, Supervision, Funding acquisition. **Laura Micheli:** Writing – review & editing, Writing – original draft, Investigation, Data curation. **Hugo R. Arias:** Writing – review & editing, Writing – original draft, Project administration, Funding acquisition, Conceptualization. **Deborah Rudin:** investigation. **Matthias E. Liechti:** investigation, data curation.

Declaration of Competing Interest

The authors declare that they have no known competing financial interests or personal relationships that could have appeared to influence the work reported in this paper.

References

[1] R.J. Yong, P.M. Mullins, N. Bhattacharyya, Prevalence of chronic pain among adults in the United States, Pain 163 (2022) e328–e332, https://doi.org/10.1097/j.pain.0000000000002291.
[2] S. Mills, N. Torrance, B.H. Smith, Identification and management of chronic pain in primary care: a review, Curr. Psychiatry Rep. 18 (2016) 22, https://doi.org/10.1007/s11920-015-0659-9.
[3] T.O. Fowler, C.O. Durham, J. Planton, B.J. Edlund, Use of nonsteroidal anti-inflammatory drugs in the older adult, J. Am. Assoc. Nurse Pract. 26 (2014) 414–423, https://doi.org/10.1002/2327-6924.12139.
[4] J.L. Cortes-Altamirano, A. Olmos-Hernandez, H.B. Jaime, P. Carrillo-Mora, C. Bandala, S. Reyes-Long, A. Alfaro-Rodríguez, Review: 5-HT1, 5-HT2, 5-HT3 and 5-HT7 receptors and their role in the modulation of pain response in the central nervous system, Curr. Neuropharmacol. 16 (2018), https://doi.org/10.2174/1570159×15666170911121027.
[5] C. Courteix, A. Dupuis, P.-Y. Martin, B. Sion, 5-HT2A receptors and pain, in: B. P. Guiard, G. Di Giovanni (Eds.), 5-HT2A Receptors in the Central Nervous System, Springer International Publishing, Cham, 2018, pp. 339–352, https://doi.org/10.1007/978-3-319-70474-6_14.
[6] Q.Q. Liu, X.X. Yao, S.H. Gao, R. Li, B.J. Li, W. Yang, R.J. Cui, Role of 5-HT receptors in neuropathic pain: potential therapeutic implications, Pharmacol. Res. 159 (2020) 104949, https://doi.org/10.1016/j.phrs.2020.104949.
[7] H. Obata, S. Saito, S. Sakurazawa, M. Sasaki, T. Usui, F. Goto, Antiallodynic effects of intrathecally administered 5-HT2C receptor agonists in rats with nerve injury, Pain 108 (2004) 163–169, https://doi.org/10.1016/j.pain.2003.12.019.
[8] A. Brenchat, X. Nadal, L. Romero, S. Ovalle, A. Muro, R. Sánchez-Arroyos, E. Portillo-Salido, M. Pujol, A. Montero, X. Codony, J. Burgueño, D. Zamanillo, M. Hamon, R. Maldonado, J.M. Vela, Pharmacological activation of 5-HT7 receptors reduces nerve injury-induced mechanical and thermal hypersensitivity, Pain 149 (2010) 483–494, https://doi.org/10.1016/j.pain.2010.03.007.
[9] R. Bardoni, Serotonergic 5-HT7 receptors as modulators of the nociceptive system, Curr. Neuropharmacol. 21 (2023) 1548–1557, https://doi.org/10.2174/1570159×21666221129101800.
[10] J. Yang, H.B. Bae, H.G. Ki, J.M. Oh, W.M. Kim, H.G. Lee, M.H. Yoon, J.I. Choi, Different role of spinal 5-HT(hydroxytryptamine)7 receptors and descending serotonergic modulation in inflammatory pain induced in formalin and

carrageenan rat models, Br. J. Anaesth. 113 (2014) 138–147, https://doi.org/10.1093/bja/aet336.
[11] P.-Y. Martin, S. Doly, A.M. Hamieh, E. Chapuy, V. Canale, M. Drop, S. Chaumont-Dubel, X. Bantreil, F. Lamaty, A.J. Bojarski, P. Zajdel, A. Eschalier, P. Marin, C. Courteix, mTOR activation by constitutively active serotonin6 receptors as new paradigm in neuropathic pain and its treatment, Prog. Neurobiol. 193 (2020) 101846, https://doi.org/10.1016/j.pneurobio.2020.101846.
[12] M. Drop, F. Jacquot, V. Canale, S. Chaumont-Dubel, M. Walczak, G. Satała, K. Nosalska, G.U. Mahoro, K. Słoczyńska, K. Piska, S. Lamoine, E. Pękala, N. Masurier, A.J. Bojarski, M. Pawłowski, J. Martinez, G. Subra, X. Bantreil, F. Lamaty, A. Eschalier, P. Marin, C. Courteix, P. Zajdel, Neuropathic pain-alleviating activity of novel 5-HT6 receptor inverse agonists derived from 2-aryl-1H-pyrrole-3-carboxamide, Bioorg. Chem. 115 (2021) 105218, https://doi.org/10.1016/j.bioorg.2021.105218.
[13] N. Mokhtar, M. Drop, F. Jacquot, S. Lamoine, E. Chapuy, L. Prival, Y. Aissouni, V. Canale, F. Lamaty, P. Zajdel, P. Marin, S. Doly, C. Courteix, The constitutive activity of spinal 5-HT6 Receptors contributes to diabetic neuropathic pain in rats, Biomolecules 13 (2023) 364, https://doi.org/10.3390/biom13020364.
[14] L.P. Cameron, R.J. Tombari, J. Lu, A.J. Pell, Z.Q. Hurley, Y. Ehinger, M.V. Vargas, M.N. McCarroll, J.C. Taylor, D. Myers-Turnbull, T. Liu, B. Yaghoobi, L. J. Laskowski, E.I. Anderson, G. Zhang, J. Viswanathan, B.M. Brown, M. Tjia, L. E. Dunlap, Z.T. Rabow, O. Fiehn, H. Wulff, J.D. McCorvy, P.J. Lein, D. Kokel, D. Ron, J. Peters, Y. Zuo, D.E. Olson, A non-hallucinogenic psychedelic analogue with therapeutic potential, Nature 589 (2021) 474–479, https://doi.org/10.1038/s41586-020-3008-z.
[15] J.A. Heinsbroek, G. Giannotti, J. Bonilla, D.E. Olson, J. Peters, Tabernanthalog reduces motivation for Heroin and alcohol in a polydrug use model, Psychedelic Med. 1 (2023) 111–119, https://doi.org/10.1089/psymed.2023.0009.
[16] H.R. Arias, D. Rudin, D.J. Hines, A. Contreras, A. Gulsevin, D. Manetti, Y. Anouar, P. De Deurwaerdere, J. Meiler, M.N. Romanelli, M.E. Liechti, A. Chagraoui, The novel non-hallucinogenic compound DM506 (3-methyl-1,2,3,4,5,6-hexahydroazepino[4,5-b]indole) induces sedative- and anxiolytic-like activity in mice by a mechanism involving 5-HT2A receptor activation, Eur. J. Pharmacol. 966 (2024) 176329, https://doi.org/10.1016/j.ejphar.2024.176329.
[17] R. Simeoli, G. Mattace Raso, A. Lama, C. Pirozzi, A. Santoro, F. Di Guida, M. Sanges, E. Aksoy, A. Calignano, A. D'Arienzo, R. Meli, Preventive and therapeutic effects of Lactobacillus paracasei B21060-based synbiotic treatment on gut inflammation and barrier integrity in colitic mice, J. Nutr. 145 (2015) 1202–1210, https://doi.org/10.3945/jn.114.205989.
[18] G.J. Bennett, Y.-K. Xie, A peripheral mononeuropathy in rat that produces disorders of pain sensation like those seen in man, Pain 33 (1988) 87–107, https://doi.org/10.1016/0304-3959(88)90209-6.
[19] S.P. Cohen, J. Mao, Neuropathic pain: mechanisms and their clinical implications, f7656–f7656, BMJ 348 (2014), https://doi.org/10.1136/bmj.f7656.
[20] L. Grundy, A. Erickson, S.M. Brierley, Visceral pain, Annu. Rev. Physiol. 81 (2019) 261–284, https://doi.org/10.1146/annurev-physiol-020518-114525.
[21] A.M. Drewes, A.E. Olesen, A.D. Farmer, E. Szigethy, V. Rebours, S.S. Olesen, Gastrointestinal pain, Nat. Rev. Dis. Prim. 6 (1) (2020), https://doi.org/10.1038/s41572-019-0135-7.
[22] L.-X. Shao, C. Liao, I. Gregg, P.A. Davoudian, N.K. Savalia, K. Delagarza, A. C. Kwan, Psilocybin induces rapid and persistent growth of dendritic spines in frontal cortex in vivo, Neuron 109 (2021) 2535–2544.e4, https://doi.org/10.1016/j.neuron.2021.06.008.
[23] A.B. Casey, M. Cui, R.G. Booth, C.E. Canal, Selective" serotonin 5-HT2A receptor antagonists, Biochem. Pharmacol. 200 (2022) 115028, https://doi.org/10.1016/j.bcp.2022.115028.
[24] J.E. Leysen, F. Awouters, L. Kennis, P.M. Laduron, J. Vandenberk, P.A. Janssen, Receptor binding profile of R 41 468, a novel antagonist at 5-HT2 receptors, Life Sci. 28 (1981) 1015–1022, https://doi.org/10.1016/0024-3205(81)90747-5.
[25] J. Lu, M. Tjia, B. Mullen, B. Cao, K. Lukasiewicz, S. Shah-Morales, S. Weiser, L. P. Cameron, D.E. Olson, L. Chen, Y. Zuo, An analog of psychedelics restores functional neural circuits disrupted by unpredictable stress, Mol. Psychiatry 26 (2021) 6237–6252, https://doi.org/10.1038/s41380-021-01159-1.
[26] H.-S. Tae, M.O. Ortells, B.J. Tekarli, D. Manetti, M.N. Romanelli, J.M. McIntosh, D. J. Adams, H.R. Arias, DM506 (3-Methyl-1,2,3,4,5,6-hexahydroazepino[4,5-b] indole fumarate), a novel derivative of Ibogamine, inhibits α7 and α9α10 nicotinic acetylcholine receptors by different allosteric mechanisms, ACS Chem. Neurosci. 14 (2023) 2537–2547, https://doi.org/10.1021/acschemneuro.3c00212.
[27] S. Irwin, Comprehensive observational assessment: Ia. A systematic, quantitative procedure for assessing the behavioral and physiologic state of the mouse, Psychopharmacologia 13 (1968) 222–257, https://doi.org/10.1007/BF00401402.
[28] L. Micheli, M. Durante, E. Lucarini, S. Sgambellone, L. Lucarini, L. Di Cesare Mannelli, C. Ghelardini, E. Masini, The Histamine H4 receptor participates in the anti-neuropathic effect of the adenosine A3 receptor agonist IB-MECA: role of CD4 + T cells, Biomolecules 11 (2021) 1447, https://doi.org/10.3390/biom11101447.
[29] R. Russo, G. D'Agostino, G. Mattace Raso, C. Avagliano, C. Cristiano, R. Meli, A. Calignano, Central administration of oxytocin reduces hyperalgesia in mice: implication for cannabinoid and opioid systems, Peptides 38 (2012) 81–88, https://doi.org/10.1016/j.peptides.2012.08.005.
[30] L. Micheli, C. Parisio, E. Lucarini, A. Vona, A. Toti, A. Pacini, T. Mello, S. Boccella, F. Ricciardi, S. Maione, G. Graziani, P.M. Lacal, P. Failli, C. Ghelardini, L.D. C. Mannelli, VEGF-A/VEGFR-1 signalling and chemotherapy-induced neuropathic pain: therapeutic potential of a novel anti-VEGFR-1 monoclonal antibody, J. Exp. Clin. Cancer Res. 40 (2021), https://doi.org/10.1186/S13046-021-02127-X.
[31] E. Lucarini, E. Pagnotta, L. Micheli, C. Parisio, L. Testai, A. Martelli, V. Calderone, R. Matteo, L. Lazzeri, L. Di Cesare Mannelli, C. Ghelardini, Eruca sativa meal against diabetic neuropathic pain: an H(2)S-mediated effect of Glucoerucin, Molecules 24 (2019), https://doi.org/10.3390/molecules24163006.
[32] L. Micheli, E. Lucarini, E. Trallori, C. Avagliano, C. De Caro, R. Russo, A. Calignano, C. Ghelardini, A. Pacini, L. Di Cesare Mannelli, Phaseolus vulgaris L. Extract: Alpha-amylase inhibition against metabolic syndrome in mice, Nutrients 11 (2019) 1778, https://doi.org/10.3390/nu11081778.
[33] E. Lucarini, C. Parisio, J.J.V. Branca, C. Segnani, C. Ippolito, C. Pellegrini, L. Antonioli, M. Fornai, L. Micheli, A. Pacini, N. Bernardini, C. Blandizzi, C. Ghelardini, L. Di Cesare Mannelli, Deepening the mechanisms of visceral pain persistence: an evaluation of the gut-spinal cord relationship, Cells 9 (2020) 1772, https://doi.org/10.3390/cells9081772.
[34] L.I. Jiang, J. Collins, R. Davis, K.-M. Lin, D. DeCamp, T. Roach, R. Hsueh, R. A. Rebres, E.M. Ross, R. Taussig, I. Fraser, P.C. Sternweis, Use of a cAMP BRET sensor to characterize a novel regulation of cAMP by the Sphingosine 1-Phosphate/G13 Pathway, J. Biol. Chem. 282 (2007) 10576–10584, https://doi.org/10.1074/jbc.M609695200.
[35] C.N. Pujol, V. Dupuy, M. Séveno, L. Runtz, J. Bockaert, P. Marin, S. Chaumont-Dubel, Dynamic interactions of the 5-HT6 receptor with protein partners control dendritic tree morphogenesis, Sci. Signal. 13 (2020) eaax9520, https://doi.org/10.1126/scisignal.aax9520.
[36] P.S. Salonikidis, M. Niebert, T. Ullrich, G. Bao, A. Zeug, D.W. Richter, An ion-insensitive cAMP biosensor for long term quantitative ratiometric fluorescence resonance energy transfer (FRET) measurements under variable physiological conditions, J. Biol. Chem. 286 (2011) 23419–23431, https://doi.org/10.1074/jbc.M111.236869.
[37] S. Prasad, E. Ponimaskin, A. Zeug, Serotonin receptor oligomerization regulates cAMP-based signaling, jcs.230334, J. Cell Sci. (2019), https://doi.org/10.1242/jcs.230334.
[38] S. López-Estévez, J.M. López-Torrellardona, M. Parera, V. Martínez, Long-lasting visceral hypersensitivity in a model of DSS -induced colitis in rats, Neurogastroenterol. \ Motil. 34 (2022) e14441, https://doi.org/10.1111/nmo.14441.
[39] J. Meffre, S. Chaumont-Dubel, C. Mannoury La Cour, F. Loiseau, D.J.G. Watson, A. Dekeyne, M. Séveno, J. Rivet, F. Gaven, P. Déléris, D. Hervé, K.C.F. Fone, J. Bockaert, M.J. Millan, P. Marin, 5-HT6 receptor recruitment of mTOR as a mechanism for perturbed cognition in schizophrenia, EMBO Mol. Med. 4 (2012) 1043–1056, https://doi.org/10.1002/emmm.201201410.
[40] K. Grychowska, G. Satała, T. Kos, A. Partyka, E. Colacino, S. Chaumont-Dubel, X. Bantreil, A. Wesołowska, M. Pawłowski, J. Martinez, P. Marin, G. Subra, A. J. Bojarski, F. Lamaty, P. Popik, P. Zajdel, Novel 1H -Pyrrolo[3,2-c]quinoline based 5-HT6 receptor antagonists with potential application for the treatment of cognitive disorders associated with Alzheimer's disease, ACS Chem. Neurosci. 7 (2016) 972–983, https://doi.org/10.1021/acschemneuro.6b00090.
[41] T.S. Jensen, N.B. Finnerup, Allodynia and hyperalgesia in neuropathic pain: clinical manifestations and mechanisms, Lancet Neurol. 13 (2014) 924–935, https://doi.org/10.1016/S1474-4422(14)70102-4.
[42] M.A. Fleming, L. Ehsan, S.R. Moore, D.E. Levin, The enteric nervous system and its emerging role as a therapeutic target, Gastroenterol. Res. Pract. 2020 (2020) 1–13, https://doi.org/10.1155/2020/8024171.
[43] E. Fiorica-Howells, R. Hen, J. Gingrich, Z. Li, M.D. Gershon, 5-HT2A receptors: location and functional analysis in intestines of wild-type and 5-HT2A knockout mice, Am. J. Physiol. Liver Physiol. 282 (2002) G877–G893, https://doi.org/10.1152/ajpgi.00435.2001.
[44] T. Okumura, T. Nozu, M. Ishioh, S. Igarashi, S. Kumei, M. Ohhira, Adenosine A1 receptor agonist induces visceral antinociception via 5-HT1A, 5-HT2A, dopamine D1 or cannabinoid CB1 receptors, and the opioid system in the central nervous system, Physiol. Behav. 220 (2020) 112881, https://doi.org/10.1016/j.physbeh.2020.112881.
[45] L. Bardin, The complex role of serotonin and 5-HT receptors in chronic pain, Behav. Pharmacol. 22 (2011) 390–404, https://doi.org/10.1097/FBP.0b013e328349aae4.
[46] A. Dogrul, M.H. Ossipov, F. Porreca, Differential mediation of descending pain facilitation and inhibition by spinal 5HT-3 and 5HT-7 receptors, Brain Res. 1280 (2009) 52–59, https://doi.org/10.1016/j.brainres.2009.05.001.
[47] C.Y. Jeong, J.Il Choi, M.H. Yoon, Roles of serotonin receptor subtypes for the antinociception of 5-HT in the spinal cord of rats, Eur. J. Pharmacol. 502 (2004) 205–211, https://doi.org/10.1016/j.ejphar.2004.08.048.
[48] G. Ji, W. Zhang, L. Mahimainathan, M. Narasimhan, T. Kiritoshi, X. Fan, J. Wang, T.A. Green, V. Neugebauer, 5-HT 2C receptor knockdown in the Amygdala inhibits neuropathic-pain-related plasticity and behaviors, J. Neurosci. 37 (2017) 1378–1393, https://doi.org/10.1523/JNEUROSCI.2468-16.2016.
[49] A.M. Jaster, H. Elder, S.A. Marsh, M. de la Fuente Revenga, S.S. Negus, J. González-Maeso, Effects of the 5-HT(2A) receptor antagonist volinanserin on head-twitch response and intracranial self-stimulation depression induced by different structural classes of psychedelics in rodents. Psychopharmacology 239 (2022) 1665–1677, https://doi.org/10.1007/s00213-022-06092-x.
[50] E. Koseli, B. Buzzi, E. Choi, T. Honaker, J. González-Maeso, J. Youkin, D. Manetti, M.N. Romanelli, H.R. Arias, M.I. Damaj, Effect Of hallucinogenic and non-hallucinogenic psychedelic analogs on chronic neuropathic pain in mice, J. Pain 24 (2023) 6–7, https://doi.org/10.1016/j.jpain.2023.02.034.
[51] G.V. Carr, L.E. Schechter, I. Lucki, Antidepressant and anxiolytic effects of selective 5-HT6 receptor agonists in rats, Psychopharmacol. 213 (2011) 499–507, https://doi.org/10.1007/s00213-010-1798-7.
[52] D. Bagdas, G. Sevdar, Z. Gul, R. Younis, S. Cavun, H.-S. Tae, M.O. Ortells, H.R. Arias, M.S. Gurun(E)-3-furan-2-yl-N-phenylacrylamide (PAM-4) decreases nociception and emotional manifestations of neuropathic pain in mice by α7

nicotinic acetylcholine receptor potentiation 43 Neurol. Res. ,2021, , 1056–1068, 10.1080/01616412.2021.1949684..
[53] F. Duhr, P. Déléris, F. Raynaud, M. Séveno, S. Morisset-Lopez, C. Mannoury la Cour, M.J. Millan, J. Bockaert, P. Marin, S. Chaumont-Dubel, Cdk5 induces constitutive activation of 5-HT6 receptors to promote neurite growth, Nat. Chem. Biol. 10 (2014) 590–597, https://doi.org/10.1038/nchembio.1547.
[54] E. Lacivita, M. Niso, M. Mastromarino, A. Garcia Silva, C. Resch, A. Zeug, M. I. Loza, M. Castro, E. Ponimaskin, M. Leopoldo, Knowledge-based design of long-chain Arylpiperazine derivatives targeting multiple serotonin receptors as potential candidates for treatment of autism spectrum disorder, ACS Chem. Neurosci. 12 (2021) 1313–1327, https://doi.org/10.1021/acschemneuro.0c00647.
[55] H.-S. Tae, M.O. Ortells, A. Yousuf, S.Q. Xu, G. Akk, D.J. Adams, H.R. Arias, Tabernanthalog and ibogainalog inhibit the α7 and α9α10 nicotinic acetylcholine receptors via different mechanisms and with higher potency than the GABAA receptor and CaV2.2 channel, Biochem. Pharmacol. 223 (2024) 116183, https://doi.org/10.1016/j.bcp.2024.116183.
[56] H.K. Romero, S.B. Christensen, L. Di Cesare Mannelli, J. Gajewiak, R. Ramachandra, K.S. Elmslie, D.E. Vetter, C. Ghelardini, S.P. Iadonato, J. L. Mercado, B.M. Olivera, J.M. McIntosh, Inhibition of α9α10 nicotinic acetylcholine receptors prevents chemotherapy-induced neuropathic pain, Proc. Natl. Acad. Sci. 114 (2017), https://doi.org/10.1073/pnas.1621433114.
[57] H.R. Arias, H.S. Tae, L. Micheli, A. Yousuf, C. Ghelardini, D.J. Adams, L. Di Cesare Mannelli, Coronaridine congeners decrease neuropathic pain in mice and inhibit α9α10 nicotinic acetylcholine receptors and CaV2.2 channels, Neuropharmacology 175 (2020) 108194, https://doi.org/10.1016/j.neuropharm.2020.108194.